Transportation Consortium of South-Central States

Solving Emerging Transportation Resiliency, Sustainability, and Economic Challenges through the Use of Innovative Materials and Construction Methods: From Research to Implementation

Assessment of Compatibility of Mineral Aggregates and Binders Used in Highway Construction and Maintenance Projects

Project No. 19BASU02

Lead University: Arkansas State University

Final Report

August 2020

Disclaimer

The contents of this report reflect the views of the authors, who are responsible for the facts and the accuracy of the information presented herein. This document is disseminated in the interest of information exchange. The report is funded, partially or entirely, by a grant from the U.S. Department of Transportation's University Transportation Centers Program. However, the U.S. Government assumes no liability for the contents or use thereof.

Acknowledgements

The authors gratefully acknowledge the funding support, which was provided by the United States Department of Transportation (USDOT) through the Transportation Consortium of the South- Central States (TranSET). The authors are also thankful to the Arkansas Department of Transportation (ARDOT), and suppliers of the materials for their technical support throughout this study. The authors also appreciate all members of the Project Review Panel (PRC) for providing their inputs throughout the duration of this project. Furthermore, the authors would like to thank the industry partners, Atlas Paving Company and Ergon Inc., for providing test materials and logistic support for this study.

TECHNICAL DOCUMENTATION PAGE

1. Project No.	2. Government Accession No.	3. Recipient's Catalog No.
19BASU02		

4. Title and Subtitle	5. Report Date
Assessment of Compatibility of Mineral Aggregates and Binders Used in Highway Construction and Maintenance Projects.	Aug. 2020
	6. Performing Organization Code
7. Author(s)	**8. Performing Organization Report No.**
PI: Zahid Hossain https://orcid.org/0000-0003-3395-564X Co-PI: Ashraf Elsayed https://orcid.org/0000-0003-1506-2784 GRA: Tandra Bagchi https://orcid.org/0000-0003-3463-1954 GRA: Sumon Roy https://orcid.org/0000-0001-6183-6619	
9. Performing Organization Name and Address	**10. Work Unit No. (TRAIS)**
Transportation Consortium of South-Central States (Tran-SET) University Transportation Center for Region 6 3319 Patrick F. Taylor Hall, Louisiana State University, Baton Rouge, LA 70803	**11. Contract or Grant No.** 69A3551747106
12. Sponsoring Agency Name and Address	**13. Type of Report and Period Covered**
United States of America Department of Transportation Research and Innovative Technology Administration	Final Research Report Aug. 2019 – Aug. 2020
	14. Sponsoring Agency Code

15. Supplementary Notes

Report uploaded and accessible at Tran-SET's website (http://transet.lsu.edu/).

16. Abstract

Stripping and delamination have been deemed as some of the major premature pavement distresses to most state Departments of Transportations (DOTs) and highway agencies including the Arkansas Department of Transportation (ARDOT). It is believed that the poor compatibility between asphalt binders and aggregates is one of the major reasons behind this. This study aims to analyze the compatibility of selected asphalt binders and aggregates used in Arkansas. Asphalt binders used in this study include PG 64-22, PG 70-22, and PG 76-22; each prepared from two different crude courses. Additionally, four different types of aggregates (sandstone, limestone, gravel, and dolomite) from four different quarries in Arkansas were evaluated in the laboratory. Selected physical and mechanical properties of the aggregates, rheological properties of the asphalt binders, surface free energy (SFE) measurements of the binders and aggregates, atomic force microscopy (AFM) analyses of binders, and limited laboratory and field performance of asphalt mixture samples were evaluated to determine the compatibility between the asphalt binders and aggregates. The findings of this study are expected to help pavement researchers and highway professionals to find suitable asphalt binder-aggregate combinations for constructing the durable pavements.

17. Key Words	18. Distribution Statement
Stripping, Pavement Durability, Compatibility, Surface Free Energy, Asphalt Binders.	No restrictions. This document is available through the National Technical Information Service, Springfield, VA 22161.

19. Security Class if. (of this report)	20. Security Class if. (of this page)	21. No. of Pages	22. Price
Unclassified	Unclassified	66	

Form DOT F 1700.7 (8-72) **Reproduction of completed page authorized.**

SI* (MODERN METRIC) CONVERSION FACTORS

APPROXIMATE CONVERSIONS TO SI UNITS

Symbol	When You Know	Multiply By	To Find	Symbol
		LENGTH		
in	inches	25.4	millimeters	mm
ft	feet	0.305	meters	m
yd	yards	0.914	meters	m
mi	miles	1.61	kilometers	km
		AREA		
in^2	square inches	645.2	square millimeters	mm^2
ft^2	square feet	0.093	square meters	m^2
yd^2	square yard	0.836	square meters	m^2
ac	acres	0.405	hectares	ha
mi^2	square miles	2.59	square kilometers	km^2
		VOLUME		
fl oz	fluid ounces	29.57	milliliters	mL
gal	gallons	3.785	liters	L
ft^3	cubic feet	0.028	cubic meters	m^3
yd^3	cubic yards	0.765	cubic meters	m^3
		NOTE: volumes greater than 1000 L shall be shown in m^3		
		MASS		
oz	ounces	28.35	grams	g
lb	pounds	0.454	kilograms	kg
T	short tons (2000 lb)	0.907	megagrams (or "metric ton")	Mg (or "t")
		TEMPERATURE (exact degrees)		
^oF	Fahrenheit	5 (F-32)/9 or (F-32)/1.8	Celsius	^oC
		ILLUMINATION		
fc	foot-candles	10.76	lux	lx
fl	foot-Lamberts	3.426	$candela/m^2$	cd/m^2
		FORCE and PRESSURE or STRESS		
lbf	poundforce	4.45	newtons	N
lbf/in^2	poundforce per square inch	6.89	kilopascals	kPa

APPROXIMATE CONVERSIONS FROM SI UNITS

Symbol	When You Know	Multiply By	To Find	Symbol
		LENGTH		
mm	millimeters	0.039	inches	in
m	meters	3.28	feet	ft
m	meters	1.09	yards	yd
km	kilometers	0.621	miles	mi
		AREA		
mm^2	square millimeters	0.0016	square inches	in^2
m^2	square meters	10.764	square feet	ft^2
m^2	square meters	1.195	square yards	yd^2
ha	hectares	2.47	acres	ac
km^2	square kilometers	0.386	square miles	mi^2
		VOLUME		
mL	milliliters	0.034	fluid ounces	fl oz
L	liters	0.264	gallons	gal
m^3	cubic meters	35.314	cubic feet	ft^3
m^3	cubic meters	1.307	cubic yards	yd^3
		MASS		
g	grams	0.035	ounces	oz
kg	kilograms	2.202	pounds	lb
Mg (or "t")	megagrams (or "metric ton")	1.103	short tons (2000 lb)	T
		TEMPERATURE (exact degrees)		
^oC	Celsius	1.8C+32	Fahrenheit	^oF
		ILLUMINATION		
lx	lux	0.0929	foot-candles	fc
cd/m^2	$candela/m^2$	0.2919	foot-Lamberts	fl
		FORCE and PRESSURE or STRESS		
N	newtons	0.225	poundforce	lbf
kPa	kilopascals	0.145	poundforce per square inch	lbf/in^2

TABLE OF CONTENTS

LIST OF FIGURES

LIST OF TABLES

ACRONYMS, ABBREVIATIONS, AND SYMBOLS

AASHTO	American Association of State Highway and Transportation Officials
AC	Asphalt Concrete
AFM	Atomic Force Microscopy
ARDOT	Arkansas Department of Transportation
ASTM	American Society for Testing and Materials
ASU	Arkansas State University
BBR	Bending Beam Rheometer
DSR	Dynamic Shear Rheometer
CR	Compatibility Ratio
DMT	Derjaguin, Muller, and Toropov
DOT	Department of Transportation
FHWA	Federal Highway Administration
HCA	Heat Cast Approach
HMA	Hot Mix Asphalt
NCHRP	National Cooperative Highway Research Program
OCA	Optical Contact Angle
OCG	van Oss, Chaudhury, and Good
PAV	Pressure Aging Vessel
PFQNM™	Peak-Force Quantitative Nanomechanical Mapping
PG	Performance Grade
PPA	Polyphosphoric Acid
WOC	Work of Cohesion
RTFO	Rolling Thin Film Oven
RV	Rotational Viscosity
S1	Source 1
S2	Source 2
SBS	Styrene-Butadiene-Styrene
SD	Sessile Drop
SFE	Surface Free Energy
SHRP	Strategic Highway Research Program
S-value	Creep Stiffness
TranSET	Transportation Consortium of South-Central States
TRB	Transportation Research Board
TSR	Tensile Strength Ratio
TTI	Texas Transportation Institute
USD	Universal Sorption Device
USDOT	United States Department of Transportation
WMA	Warm Mix Asphalt
WP	Wilhelmy Plate
%	Percent
ΔG_{dry}	Adhesion Energy under the Dry Condition
G*	Complex Shear Modulus
g/gm	Gram (Unit of weight)

hrs	Hours
Hz	Unit of Frequency used in DSR Test
in.	Inch
kPa	Kilo Pascal
L	Liter
lb	Pound
min	Minute(s)
mJ/m^2	Unit of Cohesion Energy
mm	Millimeter
MPa	Mega Pascal; Unit of DMT Modulus
m-value	Slope of the Stiffness Curve
$MgSO_4$	Magnesium Sulfate
nm	Nanometer (Unit of Surface Roughness and Deformation)
nN	Adhesion Force
°C	Degree Celsius (Unit of Temperature)
°F	Degree Fahrenheit (Unit of Temperature)
Pa.s	Pascal.sec ($N.s/m^2$) Unit of Dynamic Viscosity
psi	lb/in^2
rpm	Rotation per Minute
s	Second
Γ^-	A Mono-Polar Basic Component
Γ^+	A Mono-Polar Acidic Component
Γ^{AB}	Acid-base component of total SFE, which is geometric mean of Γ^-
Γ^{LW}	An apolar or Lifshitz-Van Der Waals Component
Γ^{total}	Total Surface Free Energy
δ	Phase Angle
ΔG_{wet}	Adhesion Energy under the Wet Condition
μm	Micrometer

EXECUTIVE SUMMARY

Premature pavement distresses such as stripping and delamination, are deemed as some of the major problems to most state Departments of Transportations (DOTs) and highway agencies including the Arkansas Department of Transportation (ARDOT). It is believed that the poor compatibility between asphalt binders and aggregates is one of the major reasons behind this. The purpose of this study to assess the compatibility of selected aggregates and asphalt binders throughout Arkansas. To fulfill the objectives of this project, a series of laboratory tests of commonly-used asphalt binders and aggregates in Arkansas were conducted and the test data were analyzed to draw meaningful conclusions and recommendations.

Besides the conventional tests, some fundamental science-based advanced tests of performance grade (PG) asphalt binders were performed in the laboratory. Asphalt binders evaluated in this study were collected from two different sources (S1 and S2). The tested binders included an unmodified (PG 64-22) and two modified (PG 70-22 and PG 76-22) binders. The additives used in the modified binders were styrene-butadiene-styrene (SBS), and a combination of PPA and SBS to prepare the PG 70-22 and PG 76-22 binders, respectively. Four types of mineral aggregates from four different quarries in Arkansas were considered in this study. Superpave tests, also known as "Binder Performance," tests, such as Rotational Viscometer, Dynamic Shear Rheometer (DSR), Rolling Thin-Film Oven (RTFO), Pressure-Aging Vessel (PAV), and Bending Beam Rheometer (BBR) were performed to evaluate the rheological properties of the tested binder samples. Furthermore, an advanced and emerging technology, Atomic Force Microscopy (AFM) tool, was also used to evaluate the microscopic morphology (roughness) and micro-mechanical properties (e.g., adhesion, DMT modulus, and deformation) of the asphalt binders at the molecular level. Physical (e.g., specific gravity, absorption), mechanical (e.g., LA abrasion, soundness test), and chemical (e.g., pH) properties tests of the aggregates were conducted in the laboratory to evaluate their durability. To predict the moisture resistance of the asphalt mixtures, the Surface Free Energy (SFE) analyses of the selected asphalt binders and aggregates have been performed. Additionally, the Texas Boiling test was conducted to determine the moisture resistance of the asphalt mixture. Finally, asphalt samples were collected from two prematurely failed existing roadways, and they were tested in the laboratory. Based on the laboratory test results of asphalt binders, aggregates, and asphalt mixtures, a Microsoft Excel-based database containing the ranks of different binder-aggregate systems was developed. The findings of this study are expected to help pavement researchers and highway professionals to find suitable asphalt binder-aggregate combinations for constructing the durable pavements.

1. INTRODUCTION

1.1. Problem Statement

The ARDOT Maintenance Division is concerned about the use of certain aggregates in asphalt concrete because of their serious durability and performance issues. In particular, aggregates originating from some quarries are suspected to be problematic and suspected to be non-compatible with some asphalt products (e.g., hot mix asphalt (HMA) and chip seals). The non-compatibility issues of these aggregates can be mitigated by selecting appropriate binder sources as they can be acidic or basic based on their crude sources (e.g., Arabian and Canadian crude). The proposed study aimed at identifying the problematic aggregates and their compatible asphalt binders through mechanistic and science-based approaches. Physical (e.g., absorption), mechanical (e.g., abrasion resistance and sulfate resistance) and chemical properties (e.g., pH) of aggregates have been evaluated in the laboratory. The compatibility of these aggregates with different binder sources has been determined by measuring their surface free energies and adhesion forces by using an Optical Contact Angle (OCA) Analyzer and an Atomic Force Microscope (AFM), respectively. A Microsoft Excel database focusing on the compatibility of the aggregate-binder systems was developed. The developed database can be followed by asphalt contractors to choose the best compatible system for building longer-lasting roadways.

1.2. Background

The performance of the asphalt-aggregate system depends on the cohesion within the asphalt binder, adhesion between the aggregates and asphalt, and degradation of the aggregates *(1)*. A degree of adhesion is normally generated when two different materials come into a molecular level contact. Several fundamental theories are available to describe the adhesive bond of the asphalt-aggregate system, and they are known as mechanical, chemical, weak boundary, and thermodynamic theories *(2-3)*. Among them, the thermodynamic theory has been followed by several researchers around the world. In the thermodynamic theory, the compatibility between an asphalt-aggregate system is assessed by considering the differences of the surface energies. Besides surface free energies, there are several other factors such as interfacial tension between the asphalt binder and the aggregate, chemical composition of the asphalt binder and the aggregate, binder's viscosity, and aggregate's porosity and surface texture that affect the adhesion of the asphalt binder to the aggregate *(4)*.

The cohesive strength of the asphalt binder and the adhesive strength between the asphalt-aggregate systems can be determined by using the surface free energy (SFE) technique at both dry and wet conditions *(5-6)*. Cheng et al. *(7)* first used the Good-van Oss-Chaudhury theory or acid-base theory to calculate the free energies of the asphalt binder and the aggregates and recommended the SFE theory. The SFE technique has been followed by several researchers including the research team of the proposed study to determine the moisture-induced damage potential of the asphalt-aggregate systems *(8-10)*. According to the acid-base theory *(11)*, the SFE of a material consists of three different components: (i) the monopolar acidic component (Γ^{+}); (ii) the monopolar basic component, (Γ^{-}); and (iii) the apolar or Lifshitz-van der Waals (Γ^{LW}) component. Total SFE is the combination of the three components and these components are also used to calculate cohesion and adhesion energies.

From discussions, it is clear that the contact angles between asphalt binder samples and reference solvents are required to calculate the wettability, the work of cohesion, the work of adhesion, and

the work of debonding. The Sessile Drop (SD) method is the easiest and the most effective method to determine the contact angle of asphalt binders among other methods (e.g., dynamic contact angle, vapor absorption, gas chromatography, and AFM). In the SD method, static contact angles of asphalt binders and aggregates are measured by using an OCA device.

Some researchers prepared SFE databases for local aggregates and asphalt binders and described their performance based on the free energy of adhesion. Cheng et al. *(7)* estimated the wetting ability of commonly available aggregates and binders in Texas. Based on wetting ability properties, these researchers ranked the tested aggregate-binder systems concerning their fatigue fracture resistance and moisture resistance. For instance, Bhasin et al. *(8)* used the SFE technique to determine the energy parameters of different asphalt mixtures to aid the selection of appropriate binders and aggregates. They developed an energy parameter chart, which was interconnected with moisture sensitivity and specific surface area of aggregates. Other researchers *(e.g., 10, 12)* used the SFE technique to evaluate asphalt binders modified with warm mix asphalt (WMA) additives and amine antistripping agents. Ghabchi et al. *(13)* used the SFE method to evaluate the moisture susceptibility of asphalt mixes containing reclaimed asphalt pavement (RAP) and different types of aggregates and asphalt binders.

2. OBJECTIVES

The primary objective of this proposed research project is to assess the durability of selected aggregates throughout Arkansas and their compatibility with asphalt binders from two different crude sources. Specific objectives of this study are given as follows:

- Evaluate physical and mechanical properties (e.g., absorption and durability) of aggregates;
- Determine surface free energies and adhesion properties of binders and aggregates;
- Recommend suitable test method(s) to screen incompatible aggregates;
- Develop a database of compatible aggregate-binder systems; and
- Rank the aggregate-binder systems based on physical, chemical, and mechanical properties.

3. LITERATURE REVIEW

The performance of the asphalt-aggregate system depends on the cohesion within the asphalt binder and the adhesion between the aggregate and asphalt binder as well as the compatibility ratio. Different methods are used for determining the SFE of various materials, such as the Wilhelmy Plate (WP) method, Sessile drop (SD) method, capillary method, ring method, drop weight method, AFM, and the nuclear magnetic resonance method *(14-15)*. The SD method for measuring the SFE components has been conducted for several studies for both asphalt binders and aggregates *(14, 16-17)*. The SD method is the easiest and the most effective method to determine the contact angle of asphalt binders among other methods (e.g., dynamic contact angle, vapor absorption, gas chromatography, and AFM).

3.1. Surface Free Energy (SFE)

The SFE can be considered as the surface tension per unit length of a solid. The SFE can be determined through contact angle measurements. Water contact angle measurement alone indicates the wetting of the solid, but the SFE is the quantitative measure of the intermolecular forces at the surface that is independent of the liquid used. By knowing the SFE of the solid, one can predict the behavior of any liquid on the surface. The SFE describes the excess energy that the surface has compared to the bulk of the material *(18)*.

3.2. Sessile Drop (SD) Technique

The sessile drop technique is a method used for the characterization of solid surface energies as well as liquid surface energies. The main principle of the method is that by placing a droplet of liquid with known surface energy, the shape of the drop, specifically the contact angle, and the known surface energy of the liquid are the parameters that can be used to calculate the surface energy of the sample. The liquid used for the test is referred to as the probe liquid, and the use of several different probe liquids is required.

3.3. Compatibility between Asphalt Binders and Aggregates

The asphalt binder and the mineral aggregates are two different materials that do not tend to adhere spontaneously at room temperature. The high viscosity of asphalt is the reason for such behavior, which obstructs its ascension by capillarity into the pores of the aggregates. Particularly, it is a matter of chemical compatibility. The asphalt binder and the aggregates are forced to combine at high temperatures during the HMA production. Once the mix returns to typical ambient temperatures, the adhesive bond between asphalt binder and aggregate is defined by their compatibility; an asphalt binder-aggregate pair with good compatibility is supposed to have better adhesion properties and to be less affected by the presence of water. This could be achieved by the proper selection of materials to be used in the asphalt mix design *(19)*.

The compatibility ratio is an important parameter to identify proper asphalt binder-aggregate combination. Recently, some researchers employed compatibility analyses to find suitable binder-aggregate systems for durable pavement construction *(14, 20-21)*.

Bahramian *(22)* researched to compare the WP method with the SD method. Three commercial bitumen binders were used in this study; all binders having a paving grade 70/100. A WP instrument was used to measure the SFE of bitumen. In this method, a thin bitumen-coated glass

was prepared and placed in an oven to decrease viscosity to a suitably low level for coating the glass slides. Water, formamide, and diiodomethane were the three probe liquids that were used for contact angle measurements. In this study, the temperature of the oven was adjusted to 135ºC (275F). The bitumen binder was placed in the oven and heated for 45 minutes to one hour. A WINDCA32 software was used to control the WP device. The corresponding advancing contact angles determined with diiodomethane, water, and formamide as the probe liquids varied between 51.6º and 78.7º, between 92.1º and 97.8º, and between 79.6º and 86.1º, respectively. While conducting the sessile drop tests, bitumen samples were prepared in the same manner as the WP method. Before coating film glasses with bitumen, the film glasses were passed through the gas flame to make sure no dust was on them. A small droplet of liquid was put on the surface of bitumen by a very accurate micropump, which was connected to a syringe located on the top of the sample. The recorded image of the droplet was analyzed by the image analyzing software. In this image analyzing processes, the software measured the contact angle and surface energy. The contact angles determined with diiodomethane, water, and formamide as the probe liquids varied between 51.8º and 66.6º, between 103.8º and 100.5º, and between 81.3º and 94.7º, respectively. After the analysis, it was reported that the Owens-Wendt model is a better model for the determination of surface energy components of bituminous binders than the acid-base model. The SD method is also reported as a faster and more convenient way to measure the surface energy components of bitumen binders than the WP method.

Hanz *(23)* researched to improve current practice by investigating different test methods to quantify moisture damage as well as to find out more efficient test methods to supplement current testing procedures. Granite, gravel, and limestone were used by these researchers. A base binder (PG 58-28), and an SBS polymer modified binder (PG 64-28) were used in this study. The first objective of this research was to evaluate the ability of the stripping test to identify moisture susceptible mixtures. The Stripping Test was conducted to measure the mass loss due to the moisture conditioning of an HMA loose mix. The second objective was the initial evaluation of the fracture energy parameter to replace the tensile strength. The researcher *(23)* compared the mechanical test parameters of fracture energy and the non-mechanical parameters such as the percent mass loss with the tensile strength testing results. The measurements of the mechanical parameters of tensile strength and fracture energy were achieved through indirect tensile strength testing by using a modified version of the ASTM D4867 procedure. In this study, Gyratory samples were cut into two-inch slices and instrumented to record both stress and strain during testing. The non-mechanical testing parameter was measured by the use of the stripping test. The test quantifies stripping using a mass loss calculation by comparing unconditioned sample weight to sample weight after mechanical agitation in a water bath of elevated temperature. The mass loss represents the stripping of the asphalt from coarse aggregate and a loss of fine aggregate/asphalt adhesion. All asphalt binders used in the HMA mixes were tested to determine the parameters of complex modulus (G*) and phase angle (δ). The cohesion of the binders was also tested by measuring the pull-off strength of the asphalt binder. All tests were performed using a dynamic shear rheometer (DSR). Based on the analysis of test results collected in this study, the stripping test on loose mixtures was able to detect the potential for weak adhesion between asphalt binders and aggregates. It was also able to identify the presence of anti-stripping additive in moisture susceptible mixes. However, high variability between test results prevents the definition of a threshold value to be used as a screening test for mixtures. Both the ASTM D4867 tensile strength

and the fracture energy tests were able to identify moisture susceptible mixes and the contribution of liquid anti-stripping additives.

Al-Rawashdeh et al. *(24)* studied WMA by using the AFM technique to investigate the effects of water on the adhesion and cohesion forces in three selected asphalt binders. The asphalt binders considered in this study were: a PG 70-22 binder, a PG 70-22 mixed with Sasol wax (at 4% by weight to make a WMA binder), and a PG 70-22 with white powdered Advera (at 5% by weight to make another WMA binder). The four different cantilever tip materials used in this study were: (1) SiO_2 coated with a carboxylic acid functional group (-COOH) to measure the cohesion forces between two asphalt molecules; (2) $CaCO_3$ (representing calcite in limestone) particle cantilever tip to measure the adhesion forces between asphalt binder molecules and an aggregate molecule; (3) Ohio limestone tip to measure the adhesion forces between asphalt binder molecules and limestone; and (4) SiO_2 particle tip (representing sandstone) to measure the adhesion forces between asphalt binder molecules and sand. Based on the results obtained by the AFM test, the adhesion/ cohesion energy of the warm mix binders was at least as great as the adhesion/cohesion energy of the hot mix binder for each tip type. Thus, the WMA additives improved the adhesion/ cohesion energy between the modified binder and the tip. Furthermore, the performance of Sasobit was higher than the performance of Advera using certain cantilever tips. When the Sasobit modified binder cooled down to room temperature, a strong, uniform crystalline structure was formed which lead to a higher bonding strength between the modified binder and the tip. Under an Ohio limestone tip, dry asphalt binder samples have shown higher adhesion energy values than the wet samples. The PG 70-22 binder modified with Sasobit or Advera was reported to be susceptible to moisture damage when mixed with limestone. The adhesion of the WMA-modified binders was stronger than that of the PG 70-22 asphalt binder. Under a $CaCO_3$ tip, dry samples have higher adhesion energy values than the wet samples with Advera and Sasobit modified asphalt binders. The adhesion of both modified binders was stronger than that of the PG 70-22 asphalt binder. Under the -COOH tip, dry samples have higher cohesion energy values than the wet samples with Advera-modified PG 70-22 asphalt binders. Based on the wet/dry ratio, it was clear that the SiO_2 (sandstone) was better than limestone in terms of providing greater adhesion energy with the binder.

Jie et al. *(15)* studied the influence of organic additives and water on the adhesion of asphalt-aggregate interface. Two types of asphalt binders (SK-70 and SK-90) and two types of aggregates (limestone and basalt) were used in this research. The organic additives were Sasobit and Rice Husk (RH), and 3% of these additives by weight were added in the asphalt matrix. The researchers conducted the SD tests for the determination of SFE components of asphalt, organic additives, and aggregates. Based on the simplified matrix formula of the Young-Dupre Equation, the SFE components of raw materials are calculated. Energy ratios were established to determine the adhesion in both dry and wet conditions. In the dry condition, it was observed that the adhesion of the asphalt-aggregate interface of asphalt containing organic additives was higher than that of the base asphalt. This is because the SFE of organic additives modified asphalts is lower than that of base asphalt. So, the stability of organic additive-asphalt-aggregate is greater than that of asphalt-aggregate. The asphalt-aggregate adhesive energies of the base asphalt, the Sasobit-modified asphalt, and the RH-modified asphalt were reduced by 10.8%, 47.9%, and 32.9%, respectively. This specifies that water has a great influence on the adhesion of asphalt-aggregate. Besides, it was found that the SK-70 is more resistant to water damage than the SK-90. The average reductions in

the adhesion of SK-70-aggregate and SK-90-aggregate interfaces were 33.4% and 27.7%, respectively. The results show that the addition of organic additives can increase the adhesion of the asphalt-aggregate interface in dry conditions. On the other hand, organic additives have hydrophobic characteristics, which decrease the adhesiveness of the asphalt-aggregate interface of the asphalt in wet conditions.

Bhasin et al. *(8)* studied the moisture sensitivity of 12 asphalt mixtures by measuring their SFE values. The mixtures were composed of three different aggregate types-RA (granite), RK (basalt), and RL (gravel), and four different types of asphalt binders: AAB-1, ABD-1, AAD-1, and AAE-1. The SFE components of the asphalt binders were determined by using the contact angle approach. A universal sorption device (USD) was used to determine the SFE components of the aggregates which were measured by adsorption isotherms of the aggregates with vapors of various probe liquids. Aggregates passing the ASTM Sieve #4 and retained on the ASTM Sieve #8 were used in conducting the USD tests. Mechanical tests were also conducted in this study on samples of asphalt mixes for each of the 12 mix designs. The same gradation was used for each aggregate in all of the 12 asphalt mixes. The optimum asphalt content for each type of mixture was determined using the Superpave gyratory compactor (SGC) at 125 design gyrations and 4% air voids. Two specimens from each mix design were tested under dry conditions, and two were tested in moisture conditions. The specimens were moisture conditioned by submerging them in deionized water under vacuum to achieve a saturation level between 70% and 80%. Two types of mechanical tests were conducted on the dry and moisture-conditioned samples at a temperature of 25°C ± 1°C. The first was the dynamic modulus test in tension. This test was conducted by applying 200 load repetitions in a haversine form at a frequency of 10 Hz. The second type of test was the dynamic creep test in tension, which was performed under a high-stress level. The effect of moisture damage on the adhesion between the asphalt binder and the aggregate is more prominently manifested in a tensile test as opposed to a compression test. The ratio of the modulus and fatigue life of the moisture conditioned sample to the modulus and fatigue life of the dry sample was used to quantify the moisture sensitivity of the asphalt mixes.

Kim et al. *(25)* used the SFE properties to predict moisture damage potential of asphalt concrete mixture under cyclic loading conditions. In this study, moisture damage based on the SFE theory, and the effects of microdamage due to the cyclic loading condition on the asphalt-aggregate system at a high temperature (40^{o}C) was investigated. The introduction of moisture in either a liquid or vapor state during the cyclic loading may be more damaging than simply the moisture conditioning to an asphalt concrete sample before testing. This difference may be due to the presence of a dynamic “network” of adhesive fracture, which potentially provides a channel for moisture movement within the sample. The researchers used two types of bitumen (AAD-1 and AAM-1) with two types of aggregates (a calcareous aggregate-limestone and a siliceous aggregate-river gravel) and two mineral fillers (a traditional limestone filler and hydrated lime). The surface area of the aggregates, which were exposed to water was used as a significant index to quantify the level of the adhesive fracture. The percent of the surface area of the aggregates that had been exposed to water during the test was successfully monitored and was used as a significant index to quantify the level of the adhesive fracture. The relation between the percentages of the surface area of the aggregate exposed to water and the number of cycles of loading assists in quantifying the adhesive fracture in the asphalt-aggregate mixture. The USD and the WP methods were used to measure the surface free energies of aggregates and asphalt, and they were used to calculate the

index. The results showed that during the moisture preconditioning (27% for limestone-AAM and 34% for Limestone-AAD), the different proportion of the surface area that had been exposed to moisture indicated that the water diffusivity of the AAD binder was greater than that of AAM. Additionally, the mixture of limestone and AAD showed a steeper slope than the mixture of limestone and AAM which meant that the adhesive bonding of AAD and limestone was weaker than the bonding of limestone and AAM, and it was related to the free surface energy measurements. The analysis of moisture damage in this study reported that stripping was composed of two mechanisms: (i) water diffusing through binder films to reach and debond part of the asphalt-aggregate interface, and (ii) the propagation of water-enhanced adhesive fracture along with the interface due to repeated loading.

4. METHODOLOGY

This chapter describes the required materials, equipment, research tools, and a brief description of the test methods employed in this study. The materials and test methods were selected based on the fulfillment of the major objectives of this study as well as their suitability in different transportation and highway agencies. As the major goal of this study was to determine the compatibility of the binder-aggregate system to find out the suitable binder-aggregate combination, importance was given to the OCA test method, its working principle, the sample preparation procedures, and the analysis of the SFE and adhesion energy between the binders and aggregates. AFM test was also employed to determine the adhesion properties of asphalt binders, in addition to the Texas Boiling test to find the stripping resistance of asphalt mixes. A flowchart with a detailed test plan is shown in this chapter.

4.1. Preparation of Test Plan

To achieve the goals of the study, extensive research was conducted to develop a systematic study plan, a detailed test matrix, and a proper methodology. A project flow diagram (Figure 1) was developed showing critical steps and associated tasks for the successful completion of the project.

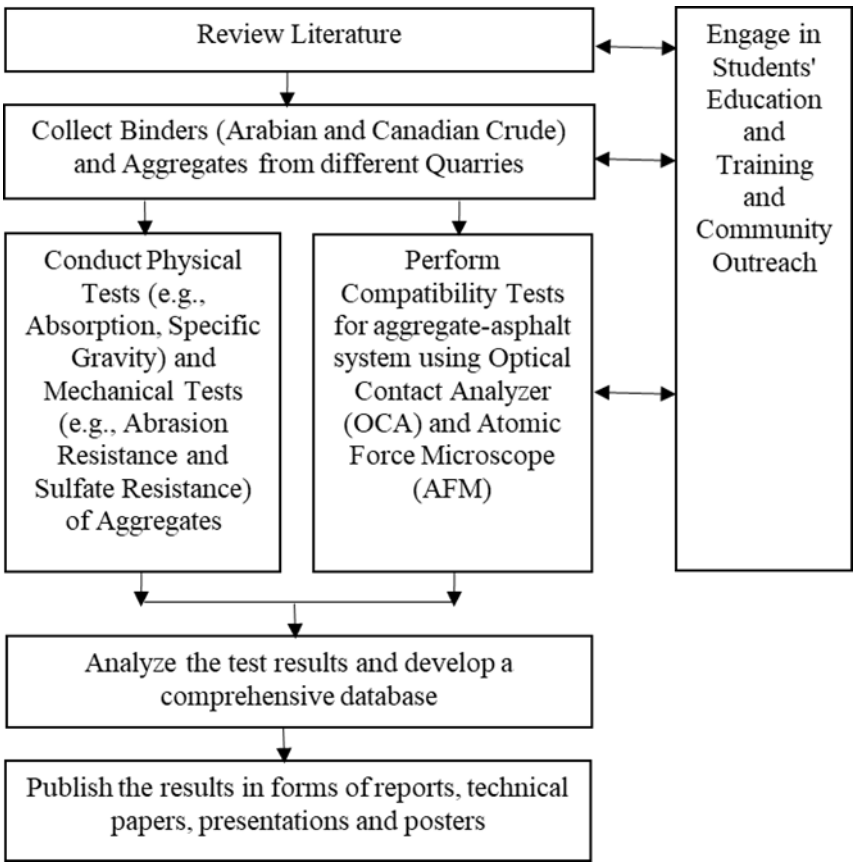

Figure 1. Project flow diagram showing the tasks.

4.2. Materials

In this study, three types of asphalt binders (PG 64-22, SBS-modified PG 70-22, and SBS plus PPA modified PG 76-22 binders) were used. These three binders were collected from two different

sources. The first binder source was a Canadian crude and manufactured by Ergon Asphalt and Emulsions, Inc. Memphis, TN. The other binder source was an Arabian crude, and it was collected from Marathon Petroleum Corporation, Catlettsburg, KY. Table 1 shows the nomenclature and flow behavior of these binder samples.

Table 1. Details of Asphalt Binder Samples Nomenclature and Properties.

Crude Source	Refinery Name	Binders	Additive	Nomenclature	Viscosity at 135°C (mPa.s)
Canadian	Ergon Asphalt & Emulsions, Inc. (Source 1)	PG 64-22	None	S1B1	504
		PG 70-22	2% SBS	S1B2	1271
		PG 76-22	2% SBS, 0.5%	S1B3	1929
Arabian	Marathon Petroleum (Source 2)	PG 64-22	None	S2B1	445
		PG 70-22	2% SBS	S2B2	1271
		PG 76-22	2% SBS, 0.75%	S2B3	1767

Four types of aggregates (e.g., Sandstone, Gravel, Limestone, and Dolomite) were collected from ARDOT approved different sources. These aggregates represent a considerable range in mineralogical and chemical compositions and durability.

Table 2. Details of Mineral Aggregate Samples.

Aggregate Type	Source
Sandstone	APAC-Central-Preston Quarry, Van Buren, AR
Gravel	Capital Quarries Company, Pocahontas, AR
Limestone	White River Materials Inc., Cord, AR
Dolomite	Capital Quarries Company, Pocahontas, AR

Furthermore, two chip seal sites were selected based on their poor performance. One site (Site 1) was in Craighead County on Highway 358 (S), and the other site (Site 2) was in Mississippi County on Highway 312. These two sites were constructed very recently, but the roadway sections became "poor" performing within a few months after the construction. Between these two sites, the visual inspection results suggested that Site 1 manifested more disintegration, raveling, and delamination compared to Site 2 even though the latter was about two years older than the former.

The chip seal samples were collected with the help and recommendations of the ARDOT District 10 engineers and crews. Firstly, a roadway section was selected where visible stripping occurred. The section was then heated up and the asphalt pavement was melted. The melted pavement was loosened from the roadway by using a shovel. Then about 20-lb. of loose sample was collected from each site for further laboratory testing. Figure 2 shows the field sample collection processes.

Figure 2. Chip seal sample collection process (a) selecting poor-performing section, (b) heating the roadway section, (c) loosened sample, and (d) collecting chip seal samples.

The details of the chip seal sample, site location, construction date, and other relevant information are presented in Table 3.

Table 3. Details of Field Samples.

Sample	Site	Construction date	Aggregate Source	Aggregate Type	Asphalt Binder source
Chip Seal 1	Site 1: Craighead Co. Line Highway 358 (S)	July 2019	Capital Quarries Company, Pocahontas, AR	Dolomite (Class 4 and Class 2 Chips)	Coastal Energy Corp.
Chip Seal 2	Site 2: Mississippi Co Highway 312	September 2017	Bradley Stone Quarry, Cord, AR	Limestone (Class 4 and Class 2 Chips)	Ergon Asphalt & Emulsions, Inc.

4.3. Laboratory Tests

Polymer modified asphalt binders and four different aggregates as well as samples from two chip seal projects were tested in the laboratory. The following tests were performed in the laboratory to achieve the goals of the project.

4.3.1. Physical Properties Test of Aggregates

Relevant physical properties (specific gravity, absorption) of the collected aggregates was determined per appropriate test methods. Specific gravity and absorption of the aggregates were determined by following AASHTO T 85.

Specific Gravity and Absorption of Aggregates: Specific gravity is critical information for the HMA Design Engineer. The value is used in calculating air voids, voids in mineral aggregate (VMA), and voids filled by asphalt (VFA). All are critical to a well-performing and durable asphalt mix. Water absorption can also be an indicator of asphalt absorption. A highly absorptive aggregate may lead to a low durability asphalt mix.

AASHTO T 85 standard was followed for determining the specific gravity and absorption of aggregates. A sample of the coarse aggregate material retained on the ASTM Sieve No. 4 (4.75 mm) was taken for this test. About 5000 g. of the coarse aggregate sample was immersed for 24 hours in a bucket. After removing the sample from the bucket, excess water from the aggregates was drained out by using an absorbent cloth to make the aggregates in saturated surface dry (SSD) condition. Then the aggregate sample was poured into a wire basket and the SSD weight of the aggregates was taken. After taking the SSD weight, the aggregates were submerged in a water bucket completely and submerged weight was taken. Finally, the sample was put into the oven at 110°C for 24 hours and the oven-dried weight was measured.

Figure 3. Specific Gravity Test of Aggregates.

4.3.2. Mechanical Properties Test of Aggregates

Abrasion resistance and sulfate resistance of aggregates considered in this study were determined per AASHTO T 96 and AASHTO T 104, respectively.

Abrasion Resistance Test of Aggregates: Abrasion resistance test is the measure of the resistance of coarse aggregates to degradation (breakdown) by impact, abrasion, and grinding. AASHTO T 96 standard was followed to perform the abrasion resistance test of the aggregates. A Type-B grade specimen was chosen for the test and a total of 5000 g. (11 lb.) of coarse aggregates was taken for the test. Of these, 2500 g. of the sample passed the ASTM 3/4″ sieve and retained on the 1/2″ sieve, and another 2500 g. passed the 1/2″ sieve and retained on the 3/8″ sieve. The sample was washed and dried in the oven for 24 hours at 110°C. The oven-dried sample was recombined and poured into the LA abrasion machine, and 11 spheres were charged in the machine. Then the machine drum was set to rotate for 500 revolutions at a constant speed of 30 to 33 rpm. After completing the desired number of rotations, the specimen was removed from the machine and sieved over ASTM Sieve No. 12. The material retained on this sieve was the intact amount. The initial mass and the intact mass were used to determine the percent loss.

Figure 4. LA Abrasion Test of Aggregates.

Sulfate Resistance Test or Soundness Test of Aggregates: The soundness test determines an aggregates' resistance to disintegration by weathering, and in particular, freeze-thaw cycles. Durable aggregates (resistant to weathering) are less likely to degrade in the field and cause premature HMA pavement distress and potentially, failure. The soundness test repeatedly submerges an aggregate sample in a sodium sulfate or magnesium sulfate solution. This process causes salt crystals to form in the aggregates' water-permeable pores. The formation of these crystals creates internal forces that apply pressure on the aggregate pores and tend to break the aggregate. After a specified number of submerging and drying repetitions, the aggregate is sieved to determine the percent loss of material.

The AASHTO T 104 method was followed to perform the soundness test. Firstly, the sulfate solution was prepared with a magnesium sulfate solution of specific gravity between 1.297 and 1.306. The sample retained on the ASTM Sieve No. 50 (0.300 mm) was thoroughly washed and dried in the oven at 230°F (110°C). Different sizes of aggregates were separated and combined the (i) 2-inch (50 mm) and 1.5-inch (37.5 mm) material to yield a 5000 g. sample, (ii) 1-inch (25.0 mm) and 0.75-inch (19.0 mm) material to yield a 1500 g. sample, and (iii) 0.5-inch (12.5 mm) and 0.375-inch (9.5 mm) material to yield a 1000 g. sample. The masses of each fractional component and the masses of each combined test sample were recorded. Each sample was placed in separate containers for the test. The samples were immersed in the prepared solution of magnesium sulfate for 16 to 18 hours. The containers were covered to reduce evaporation, prevent contamination, and maintain the temperature between 20.3 to 21.9°C for the immersion period. Afterward, the samples were removed and allowed to drain for 15 minutes. Then the samples were placed into an oven set at 230°F (110°C). The samples were allowed to dry until the change in mass was less than 0.1 percent over 4 hours (the weight was checked on four-hour intervals without letting the sample cool). After the samples reached constant mass, the samples were allowed to cool to 68 to 77°F (20 to 25°C). The immersion process was repeated five times. After the final cycle was complete, the sample was cooled and washed with water. After washing, each fraction of the sample was dried to a constant mass in an oven at 230°F (110°C). Then, the coarse material was sieved by hand with sufficient agitation only to ensure that all undersized material passes the designated sieve. The mass of the materials retained on the sieves was measured and the percent loss was determined.

Figure 5. Soundness Test of Aggregates.

4.3.3. pH Test

pH Test of Aggregates: The pH was used for the detection of the acidity of the aggregates. The standard test method ASTM D1293 was followed to measure the pH of the collected aggregates. Approximately 2000 g of coarse aggregate was taken and placed into the 1-gallon jug. An equal weight of deionized or distilled water was added to the sample, which remained there for 30 minutes. After 30 minutes, the lid was placed on the jug, and the mixture was agitated for 3 minutes. This agitation was repeated at 2 and 4-hours intervals. Upon completion of the 4-hour interval agitation, the sample was allowed to stand for 20 hours so the solids could settle out. After 20 hours, a sufficient quantity of the solution was removed and filtered through a coarse filter paper to obtain the filtered water to be tested for pH according to ASTM D1293. At first, a pH meter was calibrated with deionized water, then the filtered solution was taken in a glass container and the electrode of the pH meter was put into the water. It was stirred for a while and then waited for the pH value to be stable on the screen, and the final reading of pH was taken (Figure 6).

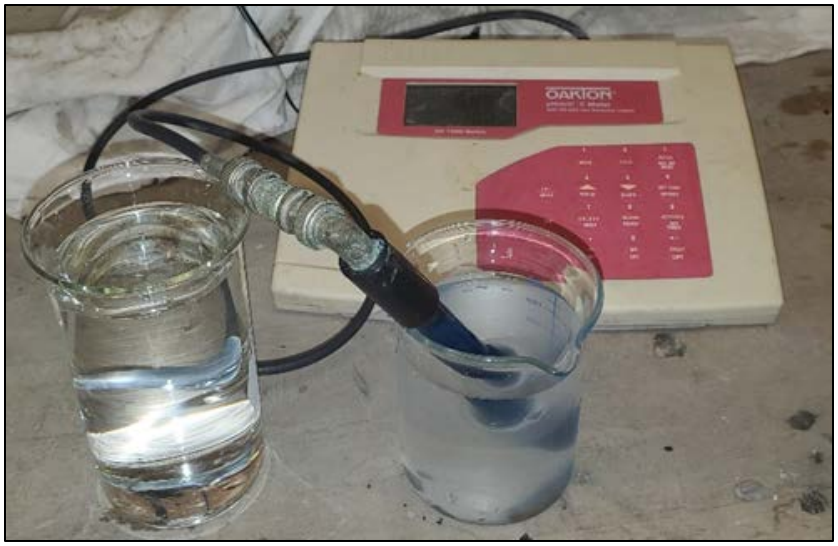

Figure 6. pH Measurement of Aggregates.

pH Test of Asphalt Binders: The acidity level of the asphalt binder was also measured in this study. For measuring the pH of a binder, a 5 g. sample binder was taken in a 250 mL beaker. Then, 30 mL of toluene was added to it. The beaker was heated slowly to dissolve the binder. The sample was allowed to cool down to room temperature and transferred to a 250 mL separatory funnel (Figure 7). After that, 15 mL of deionized water was added. Then, the separatory funnel was shaken for 2 minutes to extract the water-soluble materials from toluene into the aqueous layer. The contents of the separator funnel were centrifuged to separate the aqueous layer. The toluene layer was then poured back into the separatory funnel extracted. A pH meter (Figure 7) was used to measure the pH of the extract.

Figure 7. pH Measurement of Asphalt Binders.

4.3.4. Performance (Superpave) Tests of Asphalt Binders

To evaluate the rheological properties of asphalt binder samples, Superpave tests including Rotational Viscometer (AASHTO T 316), Dynamic Shear Rheometer (AASHTO T 315), Rolling Thin-Film Oven (RTFO) (AASHTO T 240), Pressure-Aging Vessel (PAV) (AASHTO R 28), and Bending Beam Rheometer (BBR) (AASHTO T 313) were conducted.

Rotational Viscosity (RV) Test: The viscosity of asphalt binders is the measure of the workability, pumpability, and mixability of the asphalt binders. The RV test was performed per AASHTO T 316. A DV-II+ Pro rotational viscometer (RV) from Brookfield Engineering Inc. was used to perform the test. In this research, the RV test was done from 135 °C to 180 °C at a 15 °C interval. Firstly, the asphalt binder sample was heated up to make it fluid and 10 g of heated asphalt binder sample was taken into the sample chamber. The temperature was set to the desired temperature by using a temperature controller and kept for 30 minutes to bring it to the set temperature. At that desired temperature, the asphalt binder was kept for 10 minutes to ensure the stability of the test temperature. Then, the motor was turned on and 3 different readings were taken at 1 min interval. The spindle was rotated at a constant speed of 20 rpm and the amount of torque required maintaining a constant speed (20 rpm) of the cylindrical spindle indicated the viscosity of the binder.

Figure 8. RV Test Device.

Dynamic Shear Rheometer (DSR) Test: The DSR test is performed to characterize the viscous and elastic behavior of asphalt binder by measuring the complex shear modulus (G*) and phase angle (δ) at desired temperatures and frequency of loading. The G* is the measure of the total resistance of the binder to deformation and the δ is the measure of elasticity of the binder. The lower the values of δ, the more elastic the binder is, whereas a higher value indicates viscous binder. In this research, an Anton Paar MCR 302 DSR machine was used as shown in Figure 9. For the DSR test, a thin binder sample is sandwiched between two circular plates where the lower plate is fixed and the upper plate oscillates back and forth at a certain frequency, creating a shearing action. According to AASHTO T 315, the test frequency is 10 radians per second (1.59 Hz). The test is performed according to AASHTO T 315 in different aging conditions, such as unaged, RTFO-aged, and PAV-aged, of the binders. The primary measurement according to the Superpave specification is the rutting parameter for the unaged and RTFO-aged binders, and it can be calculated by taking the ratio of G* and sinδ (i.e., G*/sinδ). On the other hand, the DSR test for PAV-aged binders calculates the fatigue factor at intermediate temperatures by multiplying G* and sinδ (i.e., G*.sinδ).

Figure 9. Dynamic Shear Rheometer.

Table 4 represents the Superpave specifications as well as rutting and fatigue factor for unaged, RTFO-aged, and PAV-aged binders.

Table 4. Superpave Specification for Rutting and Fatigue Factor.

Material	Value	Test Temperature (°C)	Specification
Unaged binder	G*/sinδ	High Service	≥ 1.0 kPa (0.145 psi)
RTFO-aged binder	G*/sinδ	High Service	≥ 2.2 kPa (0.319 psi)
PAV-aged binder	G*.sinδ	Intermediate Service	≤ 5000 kPa (725 psi)

Rolling Thin-Film Oven (RTFO): The RTFO test simulates short-term aging of asphalt binders by using high temperatures and air pressure. The aging phenomenon happens to asphalt binders during the heating and storage inside of a mixing plant is simulated by the RTFO test. Figure 10 shows an RTFO oven used for this study. The RTFO-aging of asphalt binders was done according to AASHTO T 240. Firstly, 35 g asphalt binder was poured into cleaned and preheated RTFO glass bottles. The glass bottles were then placed into the RTFO sample rack which rotated at a speed of 15 rpm. The test temperature was 163 °C, and the aging time was 85 minutes. During the test, 244 in^3/min (4 L/min) air flew into each sample bottle.

Figure 10. Rolling Thin-Film Oven (RTFO).

Pressure Aging Vessel (PAV): The PAV simulates long-term aging of asphalt binders (7 to 10 years). Figure 11 shows the PAV device used for this study and AASHTO R 28 was followed for long-term aging. The aging process was conducted at various temperatures namely, 90 °C, 100 °C, and 110 °C depending on the climatic condition.

Figure 11. Pressure Aging Vessel (PAV).

In this study, a 100 °C aging temperature was selected for PAV-aging of asphalt binders. The required air pressure 300 psi (2.07 MPa) was used for PAV-aging and the total test time was 20 hours. The PAV-residues were used for DSR tests for measuring the fatigue factor and BBR test for measuring the low temperature cracking properties of asphalt binders. However, before using the PAV-residues for any test, it is recommended to degas the sample in a vacuum degassing oven. The degassing process was done at a temperature of 170 °C for 30 minutes.

Bending Beam Rheometer (BBR) Test: Low-temperature stiffness and stress relaxation properties of asphalt binders were measured by the BBR test. These parameters indicate asphalt binders' resistance to low temperature cracking as well as provide the low service temperature of the PG grading. From the BBR test, creep stiffness and the slope of the master stiffness curve referred to as "m-value" at 60 seconds (s) are measured. The test is performed per AASHTO T 313. A typical BBR device is shown in Figure 12 and the Superpave specifications for the BBR test are presented in Table 5.

Figure 12. Bending Beam Rheometer (BBR).

Table 5. Superpave Specification for BBR Test.

Parameters	Test Temperature (°C)	Specification
"m-value" at 60 second	Low Service Temperature +10°C	≥ 0.300
Stiffness at 60 seconds	Low Service Temperature +10°C	≤ 300 MPa

The degassed PAV-aged binders are used to prepare a 0.246 x 0.492 x 5.000 inch (6.25 x 12.5 x 127 mm) solid asphalt beam for conducting this test. This beam is loaded at its midpoint in a simply supported set-up where the two supports are 4.02 inches (102 mm) apart and the load is 0.22 lb (100 g). Afterward, the beam deflection is measured at 8, 15, 30, 60, 120, and 240 seconds. Also, a stiffness master curve is plotted for these points. From the curve, slopes are drawn at 8, 15, 30, 60, 120, and 240 seconds to calculate the "m" values. The test is performed at 10 °C higher than the expected low service temperature. To simulate the low service temperature, the time-temperature superposition principle is used.

4.3.5. Sessile Drop (Optical Contact Angle) Test

The Sessile Drop test was conducted to determine the contact angles of glass coated asphalt binders with the three reference solvents (water, ethylene glycol, and formamide). The SFE parameters (work of cohesion, work of adhesion, compatibility ratio, etc.) of different aggregate and binder systems were then estimated by using the Good-van Oss-Chaudhury theory and the Young-Dupre equation. In this method, a droplet of a reference liquid was placed on a solid surface (aggregate surface or glass plate coated with asphalt binder). The shape of the drop and contact angle between the liquid and solid surface was measured by an OCA. For each drop, more than 100 contact angles on each side of the drop were measured to get a very precise measurement. The volume of the drop was regulated and the same drop volume was used for all specimens. The experimental setup of the OCA device is shown in Figure 13.

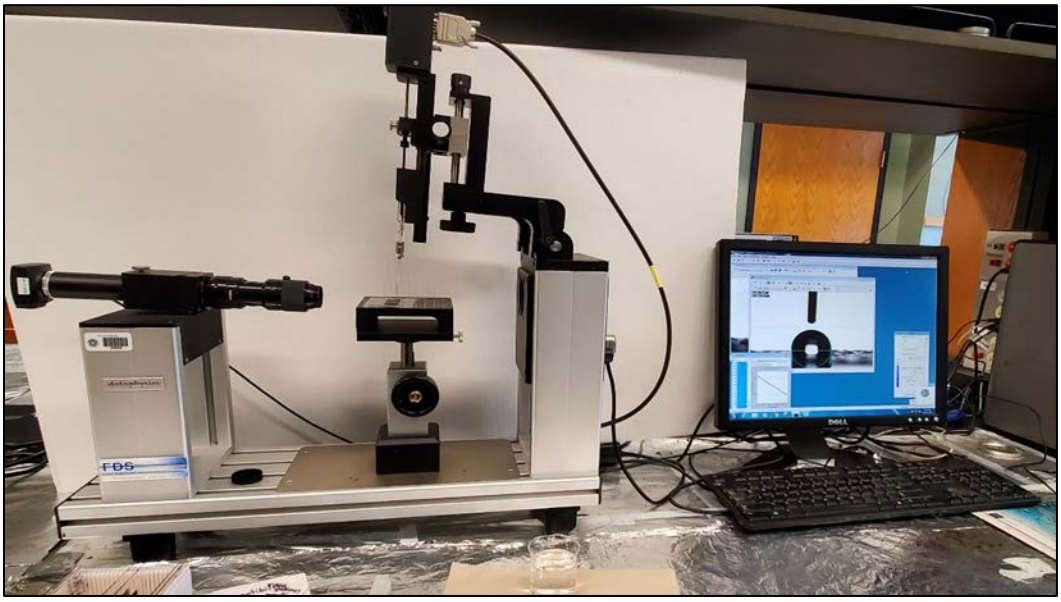

Figure 13. Experimental Setup of OCA Device.

The three different SFE components: a monopolar acidic component (Γ^+), a monopolar basic component (Γ^-), and an apolar or Lifshitz-van der Waals (Γ^{LW}) components were calculated by using the contact angles obtained from the OCA device. The acid-base component of the total SFE is denoted as Γ^{AB} and is calculated by Equation 1.

$$\Gamma^{AB} = 2\sqrt{(\Gamma^+\Gamma^-)} \quad [1]$$

The Total SFE (Equation 2) is calculated as the summation of Γ^{LW} and Γ^{AB}.

$$\Gamma^{total} = \Gamma^{LW} + \Gamma^{AB} \quad [2]$$

The Gibb's free energy of adhesion (ΔG_{ad}) consists of two components, as shown in Equation 3.

$$\Delta G_{ad} = \Delta G^{LW}_{ad} + \Delta G^{AB}_{ad} \quad [3]$$

The individual components of Equation 3 are given by Equations 4 and 5.

$$\Delta G^{AB}_{ad} = -2\ \{\sqrt{(\Gamma^+_L\ \Gamma^-_S)} + (\sqrt{(\Gamma^-_L\ \Gamma^+_S)}\} \quad [4]$$

$$\Delta G^{LW}\ ad = = -2\ \sqrt{(\Gamma^{LW}_L\ \Gamma^{LW}_S)} \quad [5]$$

Combining these equations, the Young-Dupre equation for the work of adhesion can be found, as shown in Equation 6.

$$W^a = -\Delta G^{ad} = \Gamma^{total}(1+\cos\theta) = 2\{\sqrt{(\Gamma^{LW}_L \Gamma^{LW}_s)} + \sqrt{(\Gamma^{+}_L \Gamma^{-}_s)} + \sqrt{(\Gamma^{-}_L \Gamma^{+}_s)} \quad [6]$$

where, the L and S denote liquid and solid, respectively. This equation was used for further calculation of the SFE components of the asphalt binder with a reference solvent by evaluating the contact angles (θ) using the modified asphalt binders. For measuring the three unknown free energy components of the asphalt binder, three reference solvents have been recommended by many researchers (Bhasin A. et al., 2006). Similarly, the free energy of adhesion between the asphalt binder and the aggregates in the presence of water is expressed as shown in Equation 7.

$$\Delta G^{ad}\ wet = 2\Gamma^{LW}_w + 2\sqrt{(\Gamma^{LW}_a \Gamma^{LW}_A)} - 2\sqrt{(\Gamma^{LW}_a \Gamma^{LW}_w)} - 2\sqrt{(\Gamma^{LW}_A \Gamma^{LW}_w)} + 4\sqrt{(\Gamma^{+}_w \Gamma^{-}_w)} + 2\sqrt{(\Gamma^{+}_a \Gamma^{-}_A)} - 2\sqrt{(\Gamma^{-}_a \Gamma^{+}_A)} + 2\sqrt{(\Gamma^{+}_a \Gamma^{-}_w)} - 2\sqrt{(\Gamma^{-}_a \Gamma^{+}_w)} - 2\sqrt{(\Gamma^{+}_A \Gamma^{-}_w)} \quad [7]$$

The free energy cohesion (ΔG_c), which is the creation of a unit area of a crack within a material in a vacuum condition can be determined by using Equation 8.

$$\Delta G_c = 2\Gamma^{total} \quad [8]$$

Finally, the compatibility ratio (CR) is calculated from the ratio of the work adhesion between binder and aggregate in the absence of water (ΔG_{Dry}) to the work of adhesion between binder and aggregate in the presence of water (ΔG_{Wet}). Equation 9 is used for calculating CR values.

$$CR = \Delta G_{Dry} / \Delta G_{Wet} \quad [9]$$

4.3.6. Atomic Force Microscope (AFM) Test

In recent years, the AFM technology has been used by multiple researchers in investigating the micro-morphology and micro-mechanical properties of asphalt binder *(26-31)*. In this study, a commercial AFM was used to observe the surface morphology and the mechanical properties of the asphalt binders at the molecular level. The Peak Force Quantitative Nanomechanical Mapping (PFQNM™) mode of the AFM system was used, and it provided 2-D for the surface morphology and mechanistic properties (e.g., DMT Modulus, adhesion, dissipation, deformation, and height) simultaneously. The PFQNM™ system consisted of two types of mapping: the peak force tapping, and quantitative nanomechanical mapping. The peak force tapping was similar to the tapping mode that provided the morphology and force-displacement curve. The quantitative nanomechanical mapping analyzed the force-displacement curve and provided the properties of any point in the scan area. Before nanomechanical mapping, the tip was calibrated, and the stiffness of the tip cantilever and the sharpness of the tip head were entered as some major calibration parameters. In this study, stiff probes (RTESPA™) were employed (Figure 14). First, a standard sapphire sample was used to find out the deflection sensitivity of the tip. Then, a titanium sample was used to find out the tip end radius, which was related to the penetration depth of the tip into the testing material. In this study, the following scan parameters were used: scan size of 10 um x 10 um, a scan rate of 0.500 Hz, samples/lines of 512. For each test, three replicates were tested, and average values were taken to compare the test results. After conducting the AFM scan, surface morphology, and mechanical properties of the asphalt binder were quantified using NanoScope Analyses 1.5 software.

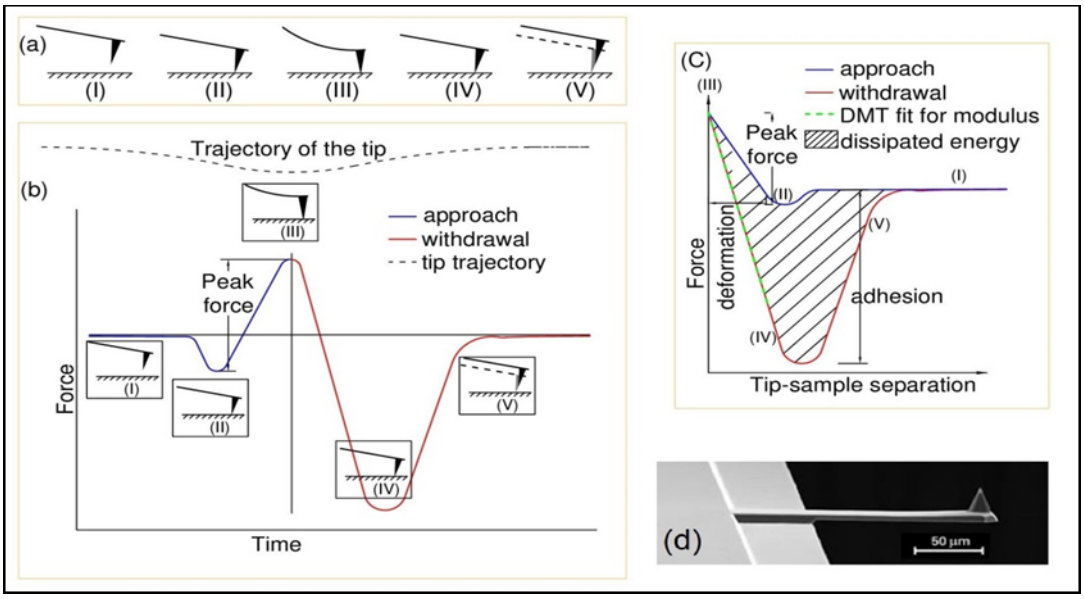

Figure 14. Working Principles of PFQNM™ Mode (27).

4.3.7. Texas Boiling Test

The Texas Boiling Test is used to evaluate the moisture susceptibility of an asphalt mix which is a simple and quick method of evaluating the moisture damage of the asphalt mixture samples. ASTM D3625 was used for conducting the Texas Boiling test. For individual aggregate mixture following aggregates could be used i) passing 3/8 inch retained on No. 4, ii) passing No. 4 retained on No. 10, iii) passing No. 10 retaining on No. 40, and iv) passing No. 40 retaining on No. 80. To evaluate the total aggregate mixture, the sample should have the same gradation as proposed for the construction work. However, the aggregates greater than 7/8 inch were normally discarded for this test.

Firstly, a 1000 mL beaker was filled with 500 mL of distilled water and heated to boiling temperature. Then the loosened mixture that was kept at room temperature was added to the boiling water. The temperature of water decreased when adding the mixture, so the heat was applied to the glass beaker at a rate so that the water was reboiled within two to three minutes. The water needed to be maintained at a medium boil for ten minutes and stirred with a glass rod at three-minute intervals. The stripped asphalt should be skimmed away by the paper towel to prevent the recoating of the aggregate. Then the water was drained out from the beaker and the wet mixture was emptied on a paper towel and allowed to dry. The final data should be taken at least half an hour after the aforementioned process. Figure 15 is a guideline given by the Texas Transportation Institute (TTI) for determining what percentage of asphalt was remaining on the surface of the aggregates, which was followed in this study.

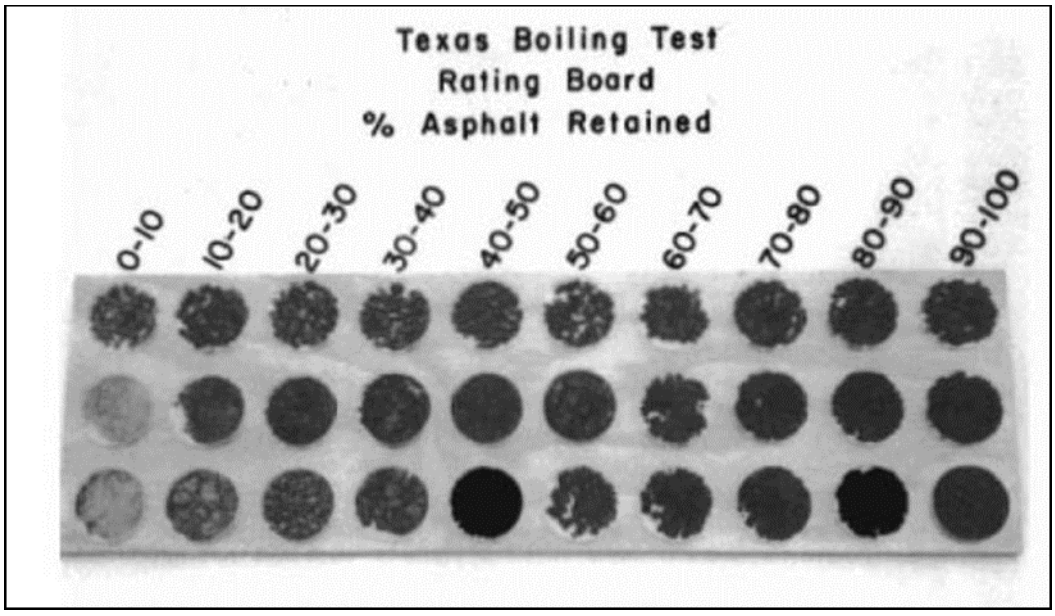

Figure 15. Rating Board for Texas Boiling Test.

4.3.8. Recovery of Residue from Emulsion

The chip seal samples were collected from the roadways and brought to the asphalt laboratory for the extraction and recovery processes. For the extraction of binder from the chip seal samples, n-Propyl Bromide (nPB) along with a centrifuge extractor was used. A rotary evaporator (Rotavapor) was used to recover the asphalt binder from the chemical solution for further testing.

The extraction procedure was done per the ASTM D6934 specification. In this method, the sample was loosened by using an oven at 110°C ± 5°C. Then 1000 g. of loose asphalt mix was then placed in the extraction bowl. A sufficient amount of nPB was poured into the bowl to fill it up and then allowed for sufficient time (not more than 1 hour) to dissolve the asphalt binder into the nPB solution. Afterward, the bowl was placed into the extractor. A 1000 mL glass beaker was placed to receive the extract binder solution. After securing the chamber cover, the extractor was started to rotate. The rotation speed was increased slowly up to 3000 rpm. The device was kept running until the extract ceased its flow from the ejection pipe. The extract of this procedure was allowed to rest for about 15 minutes to settle the fine particles, and then carefully transferred to a flask for recovery.

A rotavapor was used to recover the asphalt binder from the previously extracted nPB solution (Figure 16). The recovery procedure was performed per the ASTM D5404 specification. In this method, the rotavapor was used to evaporate nPB from the solution and subsequently cooled it down to liquid form using a condenser, leaving the asphalt binder in the original flask. At first, the flask was fitted appropriately, and the oil bath was heated at a temperature of 140 ± 3°C. The coolant was then run through the condenser while the flask was set to rotate at approximately 40 rpm. A vacuum pressure of 5.3 ± 0.7 kPa below the atmospheric pressure was applied into the flask, and nitrogen gas was supplied to the flask at a rate of approximately 500 mL/min. At these conditions, controlled evaporation of about 100 mL/min was maintained. Once the bulk amount of nPB was removed, the vacuum pressure was slowly increased up to 80.0 ± 0.7 kPa below the atmospheric pressure, and the nitrogen supply was adjusted to approximately 600 mL/min with a

rotation speed of 45 rpm. The vacuum pressure was adjusted if any foaming or bubble formation was noticed in the flask. After the formation of the last bubble, the setup was run for 10 minutes. After 10 minutes, the rotation of the flask was stopped slowly; the flask was removed and placed upside down on an appropriate size container to transfer the binder to the container. The flask-container setup was kept in an oven at a temperature of 163°C for a quick transfer of asphalt binder to the container.

Figure 16. The Rotary Evaporation System for Asphalt Binder Recovery Process.

5. ANALYSIS AND FINDINGS

5.1. Physical properties Test

5.1.1. Specific Gravity of Aggregates

Specific gravity is a measure of the density of a material compared to water. In this study, AASHTO T 85 standard was followed for determining the specific gravity and absorption of aggregates. The bulk dry specific gravity, bulk SSD specific gravity, and apparent specific gravity values of four types of aggregates are presented in Figure 17. From Figure 17, it is evident that the values of apparent specific gravity of the aggregates are higher than bulk SSD specific gravity, and the bulk SSD specific gravity is higher than bulk dry specific gravity, which is expected at all times. The values of specific gravity (bulk dry to apparent) range from 2.682 to 2.721 for limestone, 2.757 to 2.829 for dolomite, 2. 484 to 2.635 for sandstone, and 2.715 to 2.821 for gravel. Moreover, Figure 17 shows that the specific gravity values of Dolomite are the highest, whereas sandstone shows the lowest values among the four aggregates, and the gravel and limestone are in between. So, the density of sandstone compared to water is lower than the other three types of aggregates.

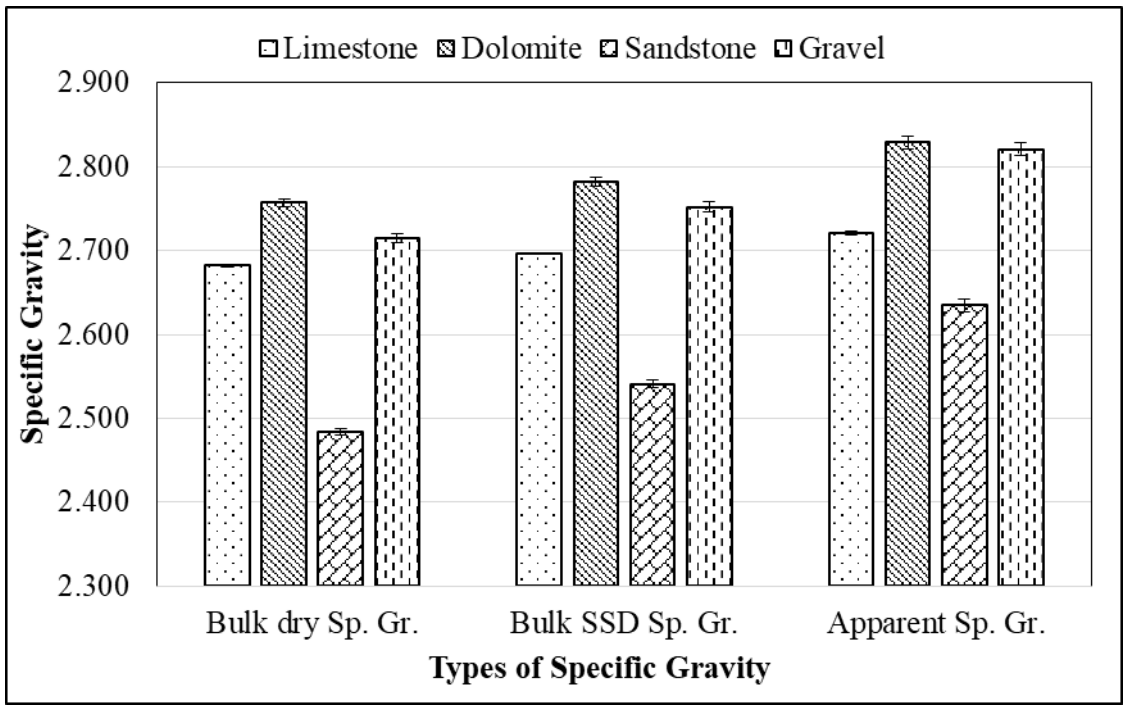

Figure 17. Specific Gravity of Aggregates.

5.1.2. Absorption of Aggregates

The absorption test was conducted along with a specific gravity test. The absorption test results of the aggregates are presented in Figure 18. According to Figure 18, it is found that the absorption of sandstone is higher than the other three types of aggregates. The absorption of sandstone is 2.3%, whereas limestone has an absorption of 0.53%, which is the lowest value among these four aggregates. It is found that the absorption of sandstone is more than four times higher than limestone. At the same time, the absorptions of dolomite and gravel are 0.92% and 1.39%,

respectively. The higher absorption of sandstone means the pavement constructed with sandstone is more moisture susceptible and stripping occurs frequently. As shown in Figure 18, limestone is more durable with respect to moisture damage, and dolomite is after that. Sandstone and gravel are less durable in this regard.

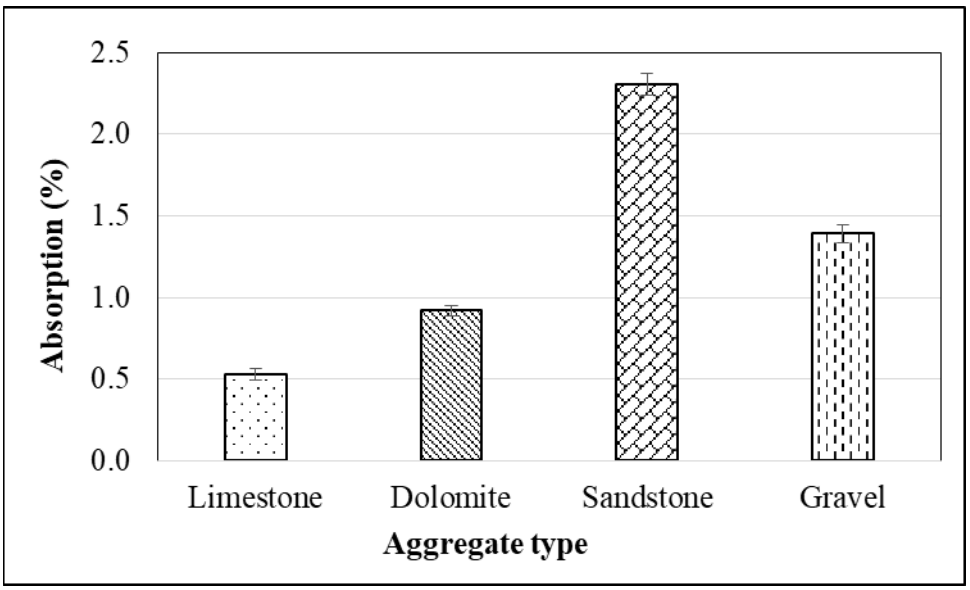

Figure 18. Absorption (%) of Aggregates.

The aggregates of the collected chip seal samples from the two field projects were recovered and tested for absorption. The absorption of the aggregates used for chip seal of Site 1 (Highway 358) and Site 2 (Highway 312) were 1.11%, and 1.59%, respectively. So, the aggregate used in Site 2 was suspected to absorb more asphalt binders and make more brittle compared to the aggregate used in Site 1. However, Site 2 deteriorated more than Site 1, which could be related to the compatibility of asphalt binder and aggregate used in these chip seal projects. The Texas Boiling test results may reveal some insights about this. It can also be mentioned that the aggregates in these existing roadways exhibited significantly higher absorption than their virgin counterpart from the same quarries. The increased absorption of aggregates in these chip seals could be related to weathering actions in their in-service condition.

5.2. Mechanical Properties of Aggregates

5.2.1. Abrasion Resistance Test Results of Aggregates

Abrasion resistance test was performed as per AASHTO T 96 to measure the resistance of coarse aggregate to degradation by impact, abrasion, and grinding. The abrasion resistance test results for the four types of aggregates are shown in Figure 19. From Figure 19, it is found that sandstone has a higher loss of 29 %, whereas gravel shows a lower percentage of loss which is only 17 %. The percent losses of dolomite and limestone are 20 % and 27 %, respectively. According to ARDOT specification, the maximum allowable loss is 40 %. In this study, the selected four aggregates meet the criteria of ARDOT. Based on the LA Abrasion test results, it is evident that sandstone is less resistant to any kind of impact, abrasion, or grinding, whereas gravel shows more resistance.

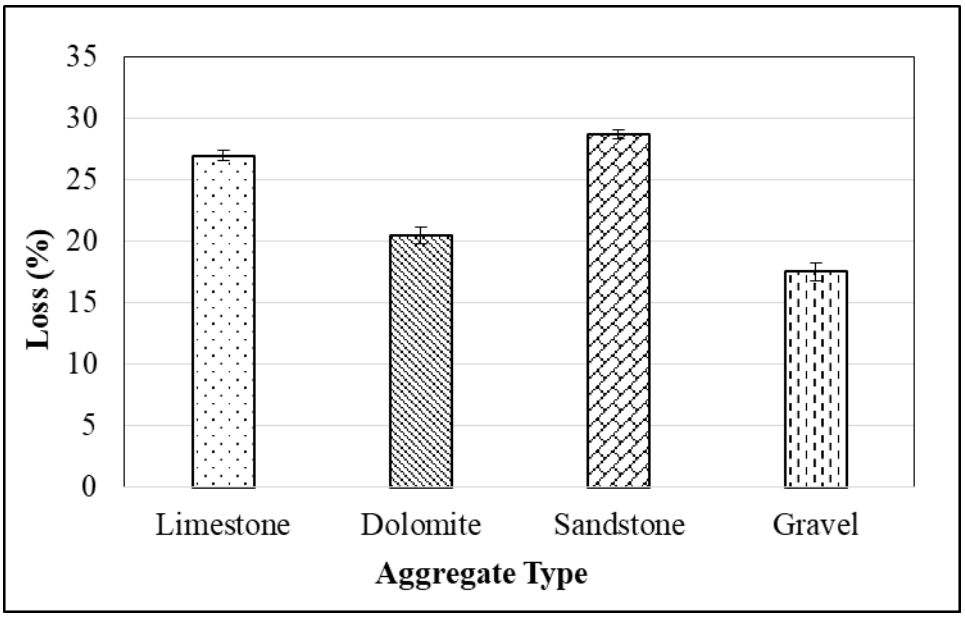

Figure 19. Percent Loss for LA Abrasion Test.

5.2.2. Sulfate Resistance Test or Soundness Test Results of Aggregates

The aggregates' resistance to disintegration by weathering, and in particular, freeze-thaw cycles was determined by conducting the soundness test. The soundness test results are shown in Figure 20. Durable aggregates (resistant to weathering) are less likely to degrade in the field and cause premature HMA pavement distresses and potentially, failure. According to the ARDOT specifications, the maximum allowable loss in the Soundness test is 12%. From Figure 20, it is found that the percentage of loss of the tested aggregates obtained from the sulfate resistance test is below the allowable limit. However, it is also observed that sandstone has the highest loss of 10.15%, which is very close to the allowable limit. At the same time, the other three aggregates observed a very low percentage of loss, ranging from 2.51 to 3.64%. Figure 20 also shows that dolomite has the least amount of percentage of loss in the Sulfate Resistance test. Based on the Sulfate Resistance test results, it is evident that sandstone is less resistant to any kind of weathering, whereas dolomite shows more resistance.

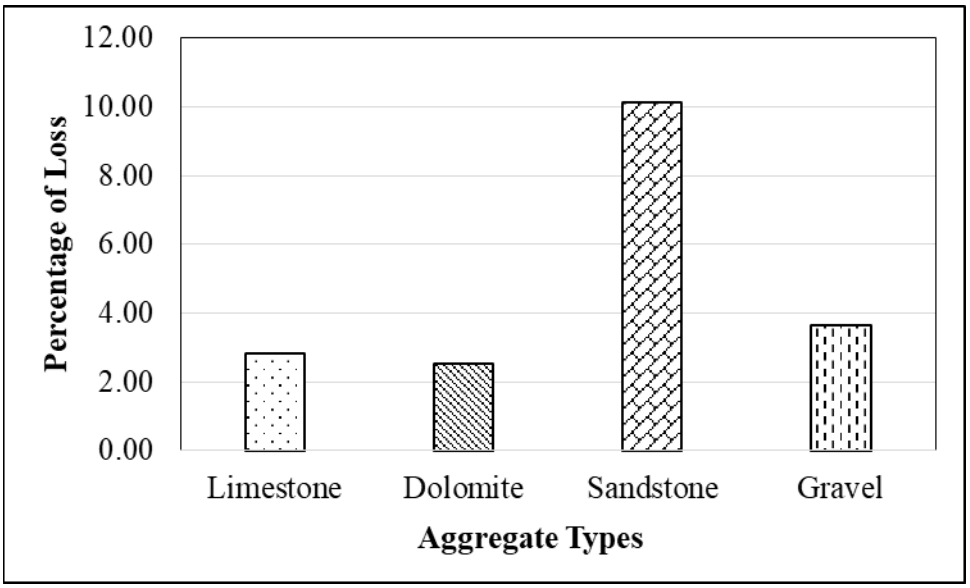

Figure 20. Soundness Test Results of Aggregates.

5.3. pH Test Results

5.3.1. pH of Aggregates

The pH of the collected aggregates was tested as per ASTM D1293 to detect the acidic or basic nature of the aggregates. Figure 21 represents the pH test results of the collected four types of aggregates. It is found that all the aggregates show the basic nature and the pH values range from 7.33 to 8.84. Among the four types of aggregates, limestone shows the highest pH value of 8.84, whereas the pH of gravel is the lowest value of 7.33. The other two aggregates, dolomite has a pH level of 8.43, and the pH of sandstone is 7.82.

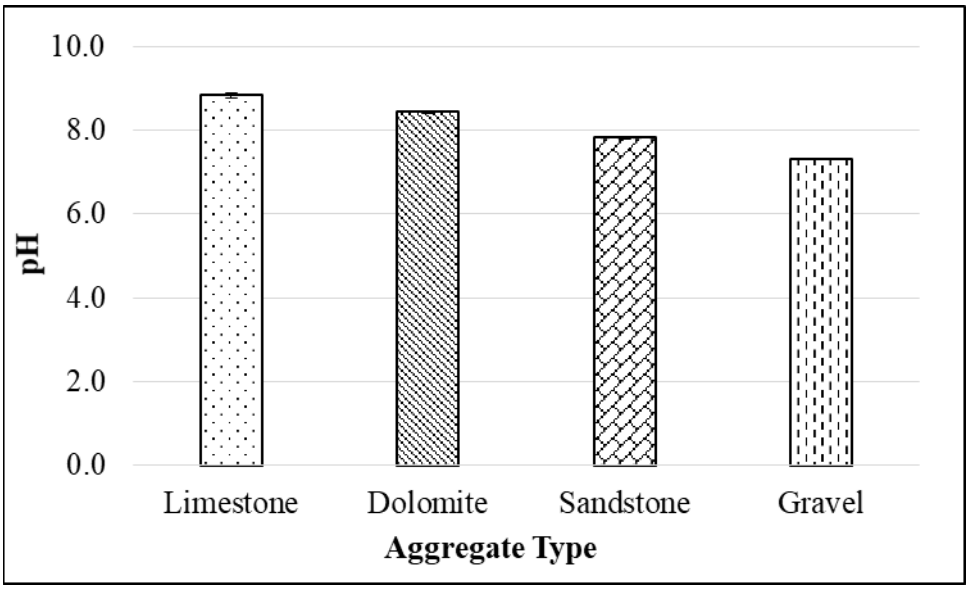

Figure 21. pH of Aggregates.

5.3.2. pH of Asphalt Binders

The pH measurements reveal that the neat binder from Source-1 was inherently basic with a pH value of 8.3. As seen in Figure 22, the pH is in recession due to the modification in a somewhat linear trend and it ends up receding below 3.0. Unlike the Source-1 binders, the Source-2 binders are acidic. The neat unmodified Source-2 binder is inherently acidic with a pH value below 7.0. It implies that the aqueous layer collected from the separatory funnel contained a higher amount of H_3O^+ ions, which results in lower pH value. On the other hand, the pH of binders modified with the combination of PPA and SBS are lower than the SBS modified binders, irrespective of their crude sources. Figure 22 indicates that the modification with SBS or PPA and SBS both increase the polar fractions within the asphalt binders. As the stiffness of an asphalt binder sample increases with its polarity *(33)*, a pH measurement test can be used as a quick tool to compare the stiffness among multiple asphalt binder samples. Though pH measurement does not tell too much about the asphalt chemistry, it helps to trace the presence of acid, and degree of modification. Since the tested asphalt binders contained PPA and SBS as modifiers and distinct pH values are observed, the highway agencies (e.g., DOTs) can run the pH test for tracing the presence of acid in asphalt binders used in their construction projects.

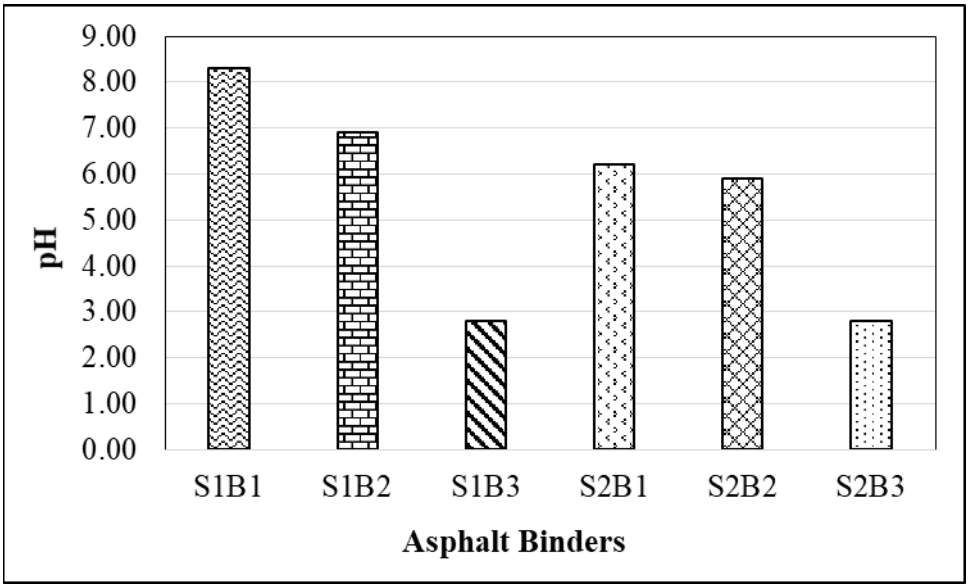

Figure 22. pH of Asphalt Binders.

5.4. Performance (Superpave) Tests of Asphalt Binders

5.4.1. Rotational Viscosity of Asphalt Binders

The RV test data shows that the binders from S2 have significantly lower viscosity values compared to their corresponding binders from S1, as presented in Table 6. Thus, S2 binders were relatively softer than S1 around mixing and compaction temperatures. It is also observed that the base binder (PG 64-22) from both sources showed the lowest viscosity among all binders used in this study. Table 6 represents that an increase in temperature decreases the viscosity of all the binders, which is expected usually. It is also found that the modification of binders makes them more viscous for both sources.

Table 6. Rotational Viscosity (mPa.s) Data of S1 and S2 Binder Samples.

Binder Type	Sample Source	At 135°C	At 150°C	At 165°C	At 180°C
S1B1	S1	504.17	254.17	145.83	75.00
S1B2	S1	1271.00	595.67	312.50	175.00
S1B3	S1	1929.33	870.67	450.00	262.50
S2B1	S2	445.83	208.33	112.50	62.50
S2B2	S2	1271.00	554.17	279.17	162.5
S2B3	S2	1767.00	758.33	350.00	187.50

The mixing and compaction temperatures for all asphalt binder samples from S1 and S2 were calculated using RV test data per the Asphalt Institute (AI). According to AI, these temperatures should be determined where the viscosity-temperature line crosses the viscosity ranges of 170 ± 20 mPa.s (mixing temperature range) and 280 ± 30 mPa.s (compaction temperature range). The method described in ASTM D2493 titled as "Standard Viscosity-Temperature Charts for Asphalts" was used to draw the viscosity-temperature line. Table 7 shows the mixing and compaction temperatures of all the binders used in this study. From Table 7, it is observed that the mixing and compaction temperatures of S1B2 or S2B2 binder (SBS-modified PG 70-22 binder) are considerably higher than those of S1B1 or S2B1. At the same time, S1B3 and S2B3 binders have the highest mixing and compaction temperatures.

Table 7. Mixing and Compaction Temperatures of unmodified and Modified Binders.

Binder Type	Sample Source	High Mixing Temperature (°C)	Low Mixing Temperature (°C)	High Compaction Temperature (°C)	Low Compaction Temperature (°C)
S1B1	S1	165	158	150	145
S1B2	S1	183	177	171	165
S1B3	S1	191	186	180	175
S2B1	S2	158	152	146	142
S2B2	S2	182	176	168	162
S2B3	S2	185	180	173	168

5.4.2. Dynamic Shear Rheometer (DSR) Test Results

In this study, DSR tests were performed in three aging conditions, namely, unaged, RTFO-aged, and PAV-aged for the characterization of the viscoelastic behavior of asphalt binders at high and intermediate service temperatures. DSR test results of unaged and RTFO-aged asphalt binders

from S1 and S2 are shown in Figures 23 through 26. Based on the results as presented in these figures, it is shown that all tested binders met the corresponding Superpave rutting factor (G*/sinδ) criteria at their high PG temperatures (G*/sinδ should be at least 1.00 kPa for unaged binders and 2.20 kPa for RTFO-aged binders). The Superpave acceptance criterion is shown with the horizontal lines in these figures. It is observed that SBS-modified unaged and RTFO-aged binders showed increased rutting factor (G*/sinδ) compared to the unmodified binders. Furthermore, PPA and SBS-modified binders indicated higher rutting resistance than the SBS-modified PG 70-22 binders which means the rutting factor increases due to modification.

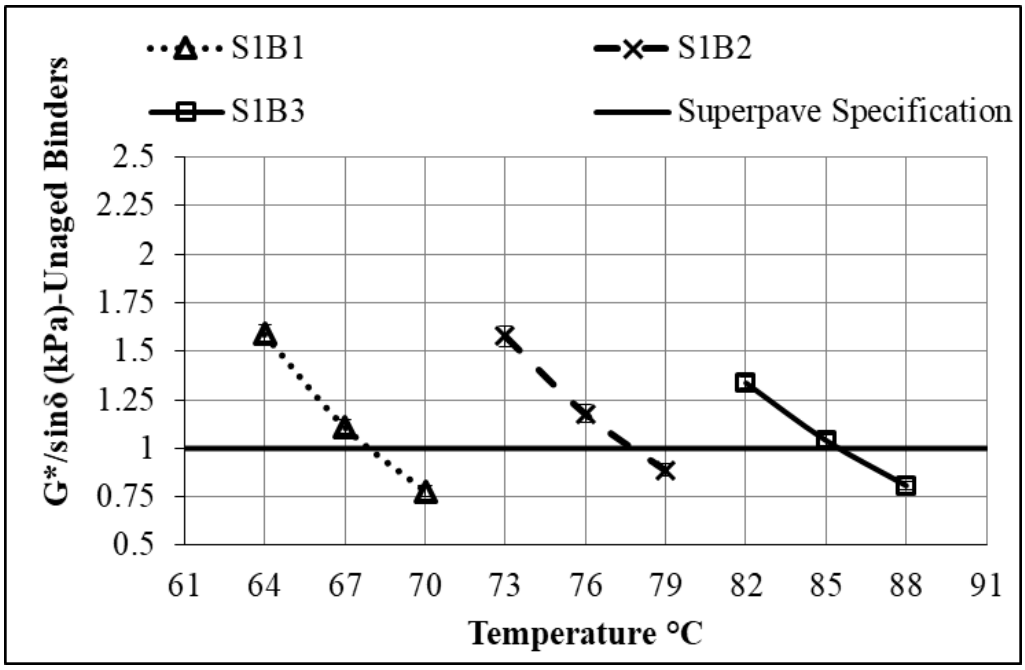

Figure 23. DSR Test Results of Unaged Asphalt Binders of Source 1.

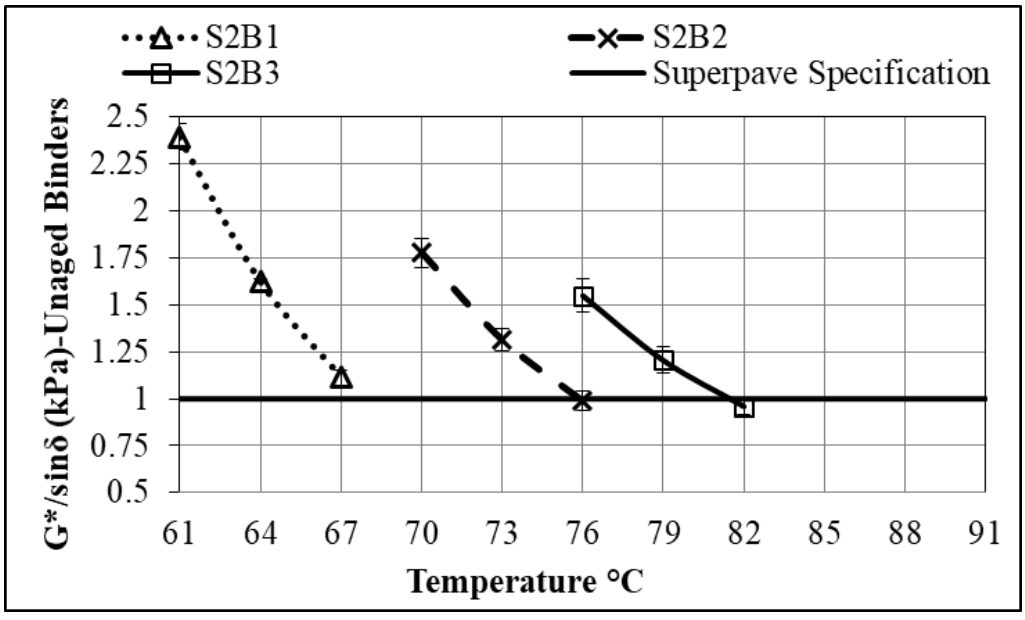

Figure 24. DSR Test Results of Unaged Asphalt Binders of Source 2.

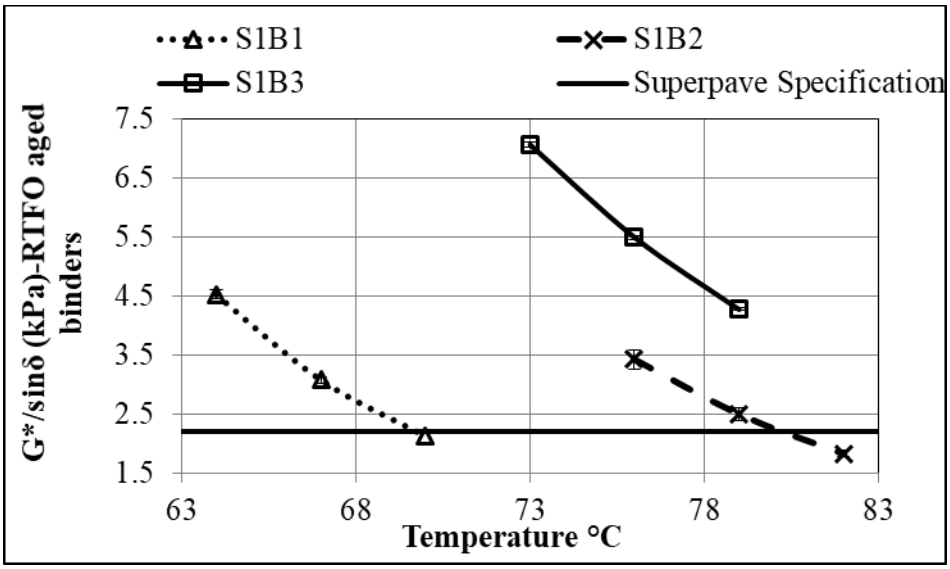

Figure 25. DSR Test Results of RTFO-aged Asphalt Binders of Source 1.

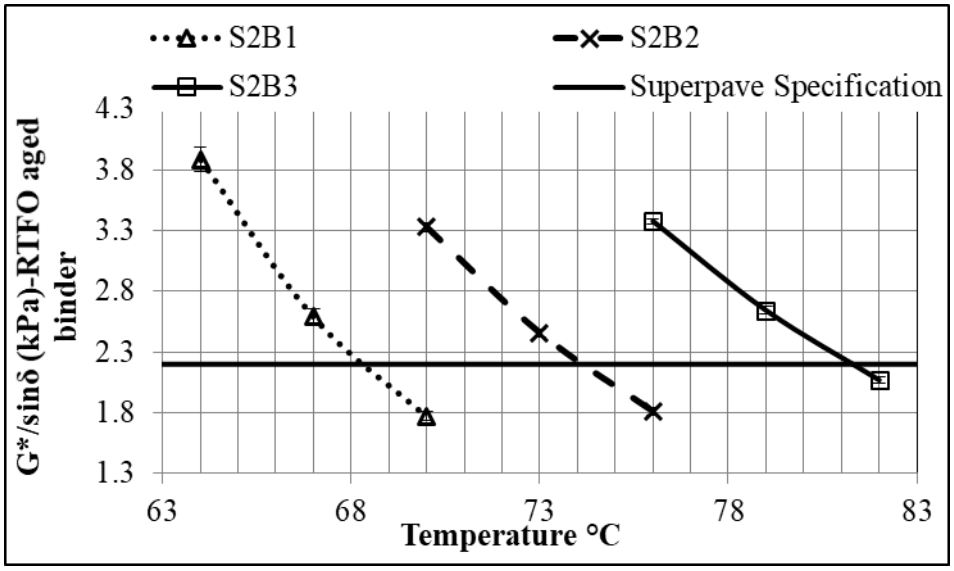

Figure 26. DSR Test Results of RTFO-aged Asphalt Binders of Source 2.

DSR test results on PAV-aged binders show fatigue characteristics of tested asphalt binders from S1 and S2 (Figures 27 through 28). As per the Superpave specifications, the G*×sinδ value of a PAV-aged binder at the intermediate temperature should not be more than 5000 kPa. The horizontal lines in these figures represent the Superpave maximum limit for fatigue resistance of binders. Test results reveal that all tested binder samples met the Superpave fatigue criterion. Test results also indicate that SBS-modified binder S1B2 are more fatigue resistant than the corresponding unmodified binder S1B1.

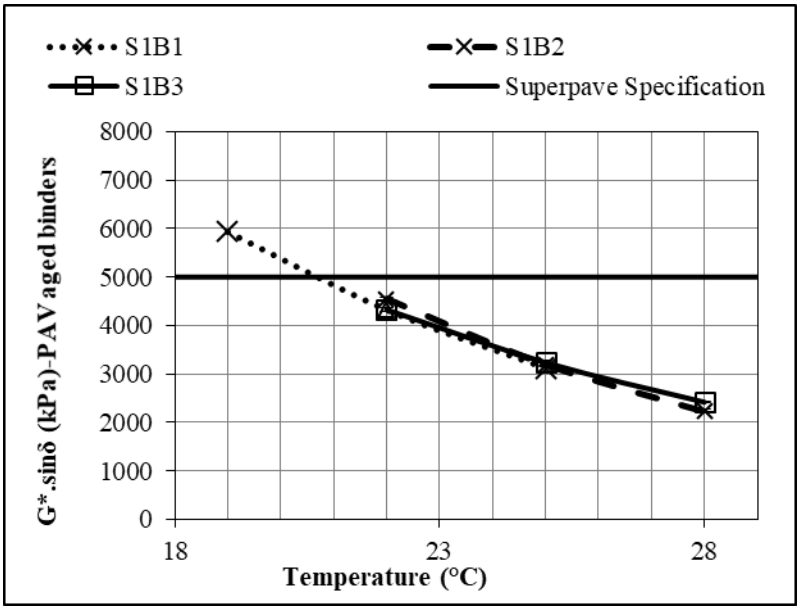

Figure 27. DSR Test Results of PAV-aged Asphalt Binders of Source 1.

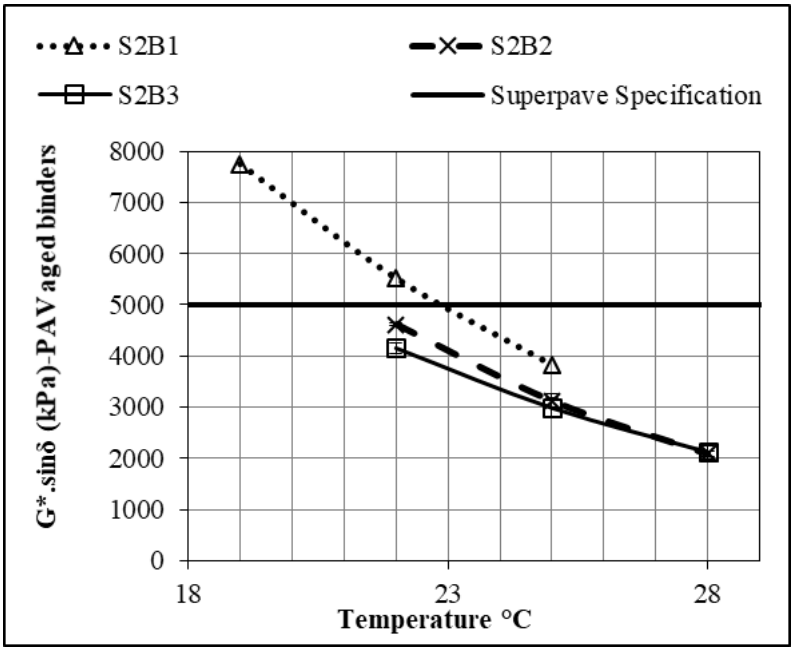

Figure 28. DSR Test Results of PAV-aged Asphalt Binders of Source 2.

5.4.3. Bending Beam Rheometer (BBR) Test Results

BBR tests were performed to measure low-temperature stiffness and stress relaxation properties of asphalt binders. From the BBR test results, S-value (creep stiffness) and m-value (the slope of the stiffness curve) were measured at 60s. According to the recommendations under the Superpave test specifications, all BBR tests were conducted at 10°C higher than the low PG temperatures of the binders in this study. For example, BBR tests were conducted at -12 °C for PG 70-22 binders. As per the requirements of the Superpave specifications, the binder's S-value should be not more than 300 MPa, and the m-value should be at least 0.300.

Figures 29 and 30 show the S-values of tested binder samples from S1 and S2. As seen from these figures, it is found that all binders met the Superpave criterion for S-value. It is observed that the lowest S-value for all binders from S1 is found for S1B3 (PPA plus SBS modified PG 76-22 binder) when then test temperature was -12 °C. For S2 binders, the lowest creep stiffness was observed for S2B2 (SSB-modified PG 70-22 binder).

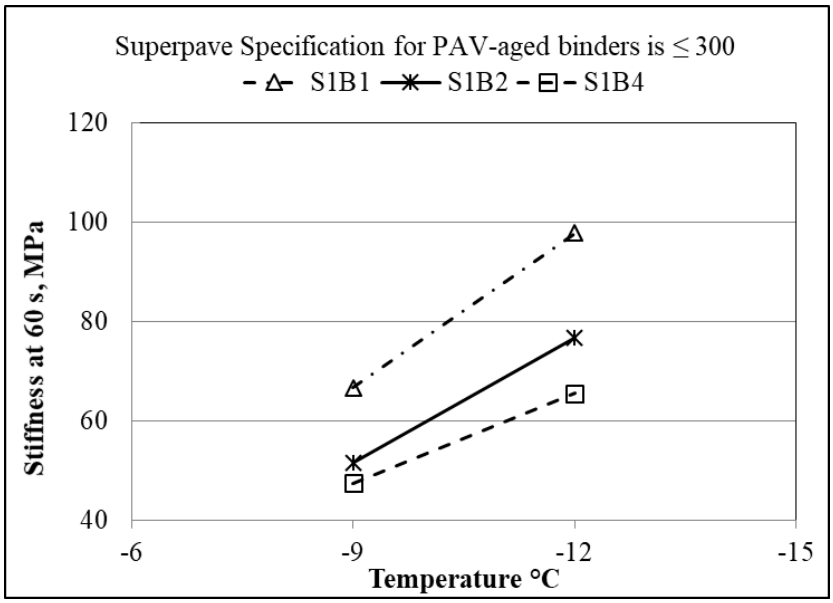

Figure 29. Creep Stiffness of the Asphalt Binders from S1.

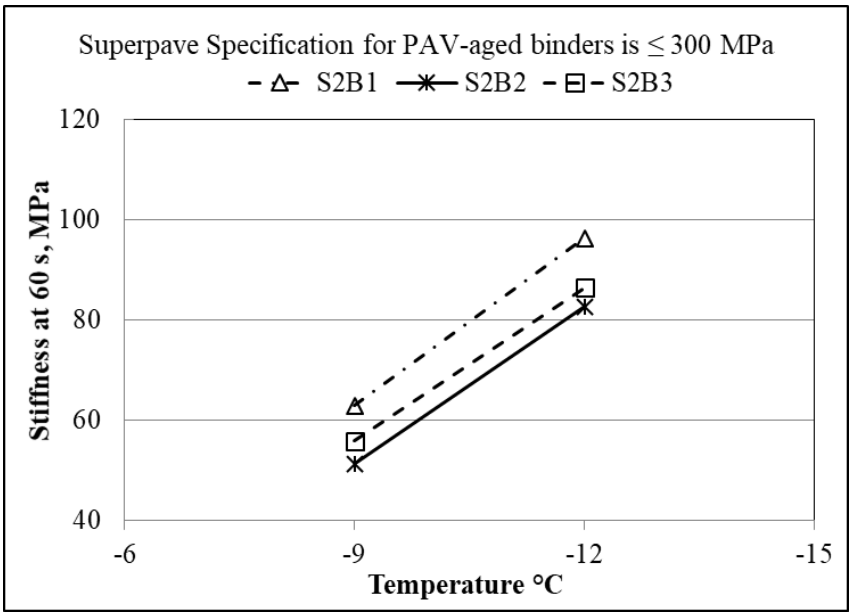

Figure 30. Creep Stiffness of the Asphalt Binders from S2.

Figures 31 and 32 show m-values of all tested binder samples from S1 and S2. From these figures, it is noted that all binder samples met the Superpave criterion for the m-value at their low PG temperature (-22°C). It is observed that the highest m-value among all S1 binders was found to be

0.4 for both S1B2 and S1B3 when the testing temperature was -12°C. It is also found that their m-values at any particular test temperature (-9°C or -12°C) are the same and overlapped with each other, shown in Figures 31 and 32. However, among all S2 binders, the highest "m" value was observed for S2B3 (PPA plus SBS-modified binder), which is found to be 0.42 at the testing temperature of -12 °C. At this testing temperature, it is also found that the lowest "m" value was observed S2B1 and S2B2 for S2.

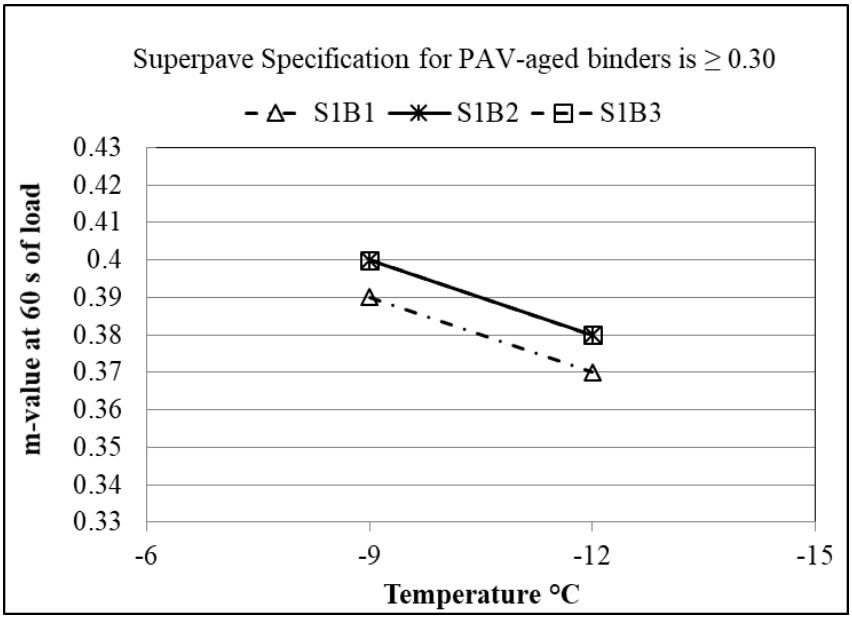

Figure 31. "m-values" of the Asphalt Binders from S1.

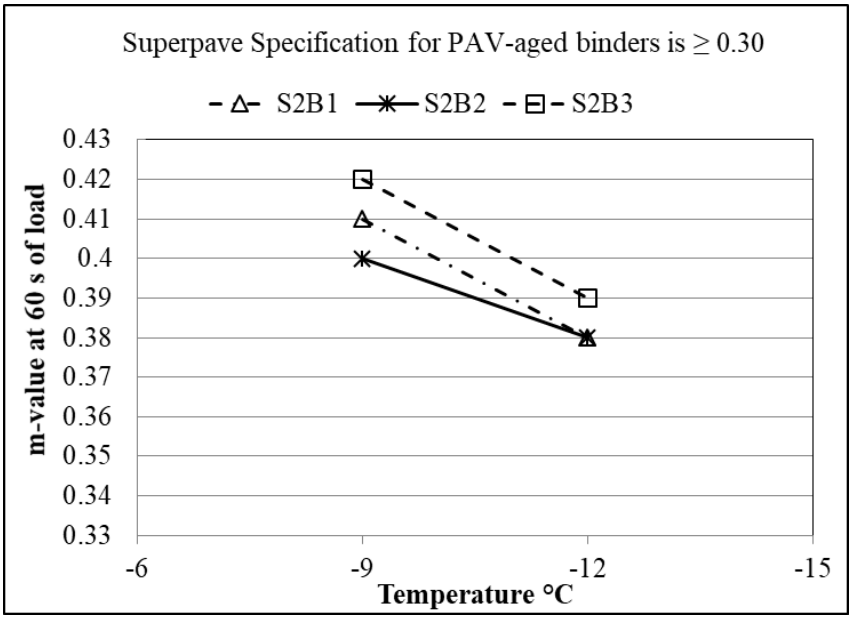

Figure 32. "m-values" of the Asphalt Binders from S2.

5.5. Sessile Drop Test Results

5.5.1. Contact Angles

The contact angle is the measure of wettability of the surface by probe liquids used for the measurement of the poor, good, and complete wetting. For the measurement of SFE, the contact angles of three different probe liquids were used as input parameters in previously described equations. The contact angles were measured using the SD technique for both asphalt binders and aggregate samples. The SD technique is based on the principle that the drop, the angle of which is measured over the sample surface is vertically symmetric, and the shape of the drop is only dictated by gravity and interfacial tension *(11)*. Literatures suggests that if the contact angle is close to zero it means the solvent is spreading on the surface properly, whereas if the contact angle is less than 90°, then the wetting is good and if it is more than 90°, then the solvent is not wetting (poor wetting) *(12, 34)*. In this study, the contact angles were measured using an OCA device. One drop of probe liquid was dropped on the asphalt binder sample, which was coated over a thin glass slide. The shape of the drop was subsequently analyzed by the SCA20 software connected to the OCA device. For one drop, more than 100 contact angles on each side of the drop were measured to get a very precise measurement. The volume of the drop was regulated, and the same volume was used for all the samples. In this study, the dosing volume was 3.5 µL, and the dosing rate was 2.0 µL/s. Separate sample preparation techniques were used for asphalt binders and aggregate samples to measure their respective contact angles *(35-38)*. The same OCA device was also used to measure the contact angles of the aggregate samples that had been used for this study.

Tables 8 through 11 show the contact angles of unaged, RTFO-aged, and PAV-aged asphalt binder and aggregate samples, respectively. Among the three probe liquids, water shows the highest contact angles than ethylene glycol or formamide.

Table 8. Contact Angles (degree) of Unaged Asphalt Binders.

Asphalt Binders (Unaged)	Water	St. Deviation	Ethylene glycol	St. Deviation	Formamide	St. Deviation
S1B1 (PG 64-22)	101.1	0.12	92.5	0.45	87.1	0.67
S1B2 (PG 70-22)	92.5	0.38	72.5	0.79	76.2	0.36
S1B3 (PG 76-22)	89.5	0.47	73.9	0.42	75.5	0.72
S2B1 (PG 64-22)	96.3	0.63	74.6	0.65	77.6	0.93
S2B2 (PG 70-22)	95.7	0.52	72.3	0.35	77.5	0.53
S2B3 (PG 76-22)	94.2	0.55	75.0	0.97	81.1	0.86

From Tables 8 through 10, it is found that the contact angles increase due to aging. For the S1B1 binder, the contact angles for water under unaged, RTFO-aged, and PAV-aged conditions are 101.1°, 102.3°, and 103.8°, respectively. This increasing trend is also observed for other asphalt binders. When a binder ages, it becomes more viscous and less fluid, and therefore the wettability of that binder also decreases, which results in an increase in the contact angle.

Table 9. Contact Angles (degree) of RTFO-aged Asphalt Binders.

Asphalt Binders (RTFO-aged)	Water	St. Deviation	Ethylene glycol	St. Deviation	Formamide	St. Deviation
S1B1 (PG 64-22)	102.3	0.51	93.3	0.42	89.9	0.18
S1B2 (PG 70-22)	101.6	1.63	89.2	1.06	86.4	0.34
S1B3 (PG 76-22)	102.1	1.36	86.5	0.74	88.8	0.88
S2B1 (PG 64-22)	101.3	0.40	92.0	0.65	85.6	0.78
S2B2 (PG 70-22)	98.5	0.29	84.3	0.58	79.9	0.56
S2B3 (PG 76-22)	98.8	1.21	82.6	0.79	80.5	0.33

Table 10. Contact Angles (degree) of PAV-aged Asphalt Binders.

Asphalt Binders (PAV-aged)	Water	St. Deviation	Ethylene glycol	St. Deviation	Formamide	St. Deviation
S1B1 (PG 64-22)	103.8	0.17	93.6	0.71	90.3	1.22
S1B2 (PG 70-22)	103.1	0.71	90.5	1.39	90.1	0.71
S1B3 (PG 76-22)	102.1	1.35	88.6	0.22	88.9	1.33
S2B1 (PG 64-22)	101.6	0.21	91.9	0.08	85.3	0.71
S2B2 (PG 70-22)	100.6	1.01	87.9	0.97	84.0	0.95
S2B3 (PG 76-22)	100.2	0.33	84.1	0.74	82.8	1.41

Table 11 shows the contact angles of the collected four types of aggregates. The collected larger size rocks were cut into small pieces, and a smooth surface was prepared by using sandpaper. Then the rock samples were washed and dried in the oven at 105°C. After preparing the rock sample, it was tested for contact angle in the OCA device, and the same three probe liquids were used for contact angle measurement. For the measurement of aggregates' contact angles, the dosing volume was 4.0 µL and the dosing rate was 2.0 µL/s. Table 11 shows that the contact angle for water is higher for sandstone and the lower value is found for dolomite. Similarly, for ethylene glycol and formamide, the highest contact angles are observed for sandstone. But for ethylene glycol, the lowest value is found for limestone. Table 11 also represents the standard deviation of the measured contact angles, and it is evident that the deviation is very low for all the measurements.

Table 11. Contact Angles of Aggregates.

Aggregate Samples	Water	St. Deviation	Ethylene glycol	St. Deviation	Formamide	St. Deviation
Sandstone	42.6	0.66	29.5	0.71	22.7	1.05
Gravel	34.6	0.74	19.0	0.87	16.9	0.90
Dolomite	20.7	1.33	18.1	0.22	16.6	0.50
Limestone	29.6	0.41	18.0	1.25	17.1	1.64

5.5.2. Surface Free Energy (SFE) Components

The SFE governs the adhesive bond strength between the asphalt binder and the aggregate as well as the cohesive bond strength of the asphalt binder. Using the contact angles, the SFE parameters are calculated. Table 12 presents the SFE components, total SFE, and work of cohesion of all the tested asphalt binders. The Lifshitz-van der Waals, Lewis acid, and Lewis base SFE components of asphalt binders play a critical role in the adhesion and cohesive bonding in the asphalt-aggregate mixture system. The quantitative information of these components is needed to estimate bond energies and to evaluate the moisture resistance of the AC mixture. It is found that the value of the Lifshitz-van der Waals component (Γ^{lw}) is higher than the acid (Γ^{+}) and base (Γ^{-}) components. For the unaged S1B1 binder, the Γ^{lw} component is 9.88, whereas the acid component is only 1.82, and the base component is 2.47. Table 12 also represents that the values of acid and base component increase with the modification of binders. Another interesting finding from Table 12 is that the total SFE is gradually decreasing due to the aging of the binders. For the unaged S1B2 binder, the value of total SFE is 14.12; it decreases to 12.05 for RTFO-aging and 11.25 for PAV-aging. The same trend is found for work of cohesion as well. Due to aging, the binders become stiffer; thus, the work of cohesion decreases.

Table 12. SFE Components of Asphalt Binders under Different Aging Conditions

Asphalt Binder Sample	Aging Condition	Γ^{lw}	Base Γ^{-}	Acid Γ^{+}	Γ^{AB}	Total SFE Γ	Γ^{+}/Γ^{-}	Cohesion (mJ/m^2)
S1B1	Un-aged	9.88	2.47	1.82	4.24	14.12	0.74	28.24
S1B2	Un-aged	6.84	4.91	5.13	10.04	16.88	1.04	33.76
S1B3	Un-aged	7.35	5.57	5.78	11.35	18.70	1.04	37.40
S2B1	Un-aged	6.23	4.11	4.36	8.47	14.70	1.06	29.39
S2B2	Un-aged	6.32	4.23	4.47	8.70	15.02	1.06	30.03
S2B3	Un-aged	6.55	4.53	4.77	9.30	15.85	1.05	31.69
S1B1	RTFO	9.81	2.31	1.64	3.89	13.70	0.71	27.41
S1B2	RTFO	5.90	2.77	3.41	6.15	12.05	1.23	24.09
S1B3	RTFO	5.74	2.84	3.22	6.05	11.79	1.13	23.58
S2B1	RTFO	5.55	3.15	3.44	6.58	12.13	1.09	24.27
S2B2	RTFO	5.90	3.67	3.93	7.60	13.50	1.07	26.99
S2B3	RTFO	5.85	3.61	3.87	7.48	13.33	1.07	26.65
S1B1	PAV	5.23	2.69	3.00	5.68	10.91	1.11	21.81
S1B2	PAV	5.31	2.82	3.12	5.94	11.25	1.11	22.50
S1B3	PAV	5.43	2.99	3.28	6.26	11.69	1.10	23.38
S2B1	PAV	5.49	3.08	3.36	6.43	11.92	1.09	23.85
S2B2	PAV	5.61	3.26	3.54	6.79	12.40	1.09	24.81
S2B3	PAV	5.67	3.35	3.62	6.96	12.63	1.08	25.27

Total SFE is the combination of the acid, base, and Lifshitz-van der Waals components. Figure 33 shows the SFE components of unaged asphalt binders from sources 1 and 2. It is observed that the S1B3 binder has the highest value of total SFE among the six binders from both sources. Among source 2 binders, PPA and SBS modified S2B3 has the highest value of total SFE. Figure 33 also

depicts that the unmodified S1B1 binder has the lowest value of total SFE. At the same time, unmodified S2B1 has a lower value of total SFE. From Figure 33, it is evident that the SFE components increase with the modification of asphalt binders.

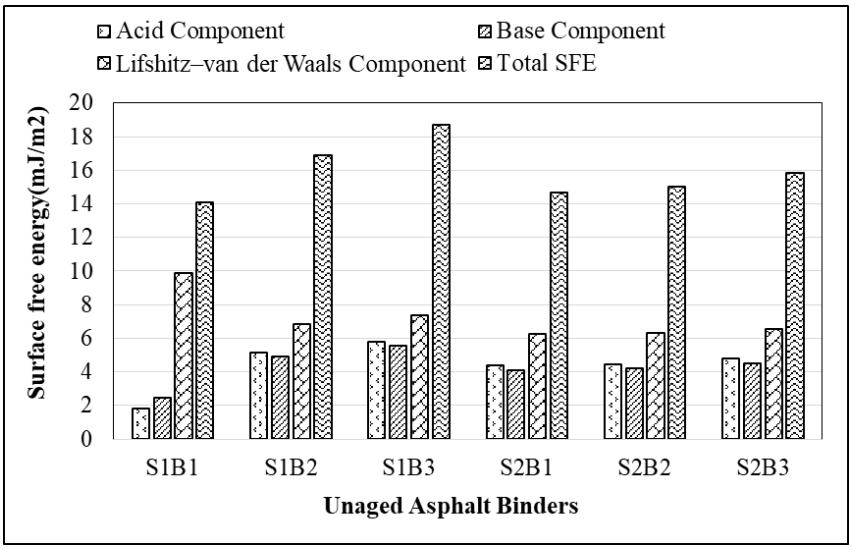

Figure 33. SFE Components of Unaged Asphalt Binders.

Figure 34 shows the SFE components of RTFO-aged asphalt binders from Sources 1 and 2. It is observed that the S1B1 binder has the highest value of total SFE among the six binders from both sources. Among source 2 binders, SBS modified S2B2 and unmodified S1B1 have the highest values of total SFE. For source 2 binders, the total SFE increases with binder modification, which was also found for unaged binders. However, source 1 RTFO-aged binders show slightly different results.

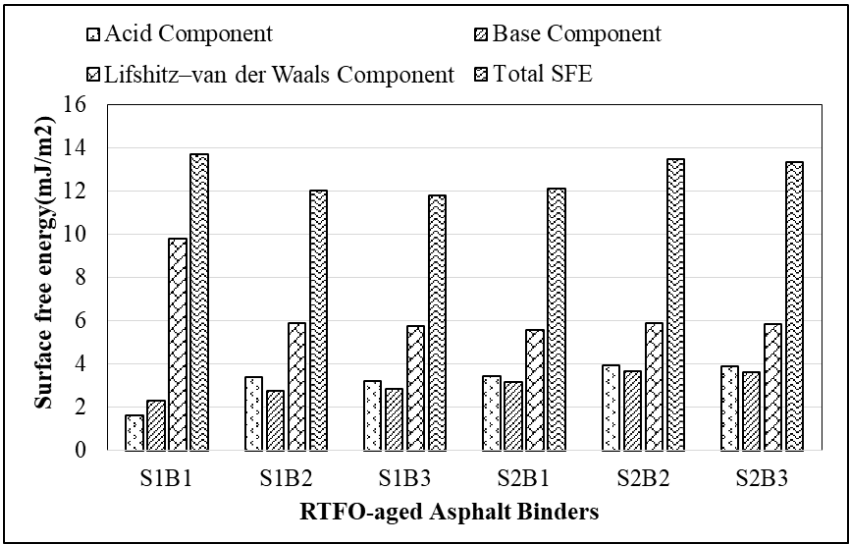

Figure 34. SFE Components of RTFO-aged Asphalt Binders.

Figure 35 represents the SFE components and total SFE of PAV-aged asphalt binder from both sources. Similar to unaged and RTFO-aged binders, PAV-aged binders also show an increasing

trend of total SFE due to the modification of binders. Among the six binders, S2B3 has the highest value of total SFE. At the same time, S2B2 and S1B3 have a higher value of total SFE.

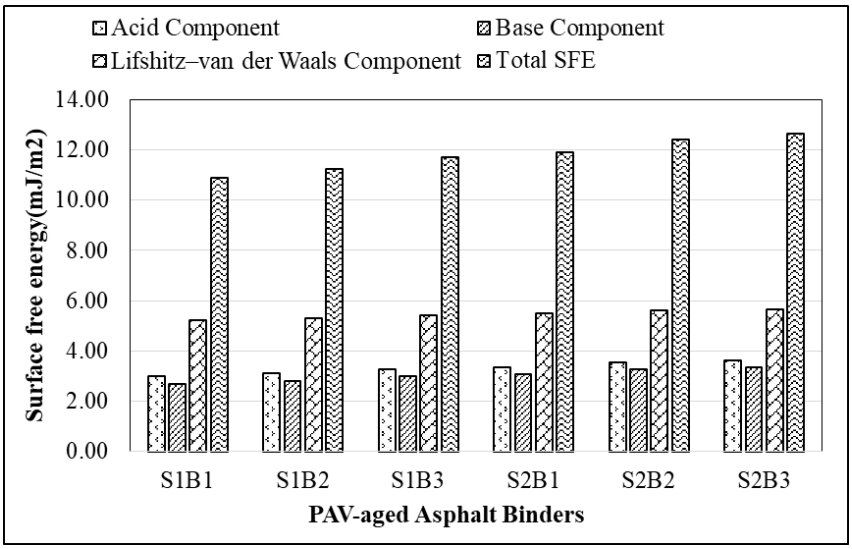

Figure 35. SFE Components of PAV-aged Asphalt Binders.

The SFE components of the collected aggregates are shown in Figure 36. Among the four aggregates, dolomite has the highest total SFE, and sandstone has the lowest value. Limestone and gravel are in between them. From Figure 36, it is found that the values of total SFEs are 90.46, 84.13, 79.22, and 70.15 for dolomite, limestone, gravel, and sandstone, respectively. Total SFE is an important parameter for binder aggregate combination. The higher value of SFE means it has a higher value of adhesion with asphalt binders, which represents a higher compatibility ratio and less moisture susceptible. Based on the test results from Figure 36, it can be said that sandstone and any binder combination will face more moisture-induced damage than the other three types of aggregates.

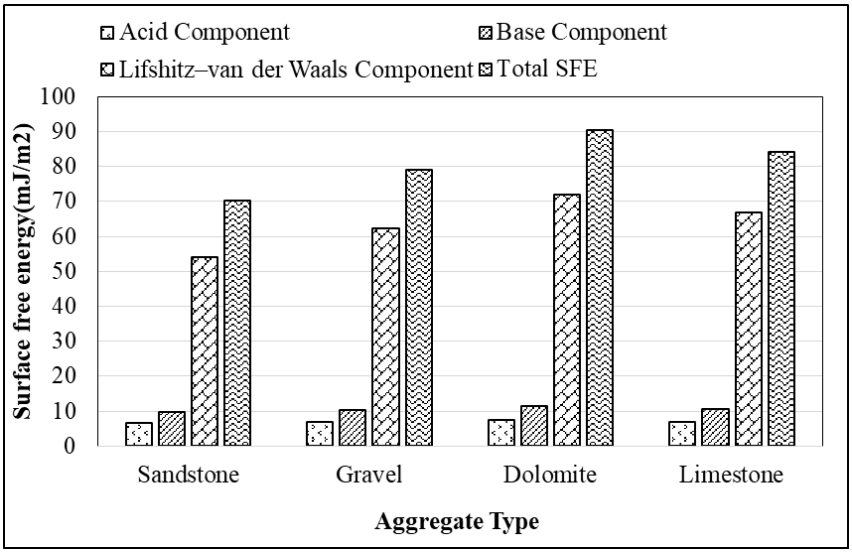

Figure 36. SFE Components of Aggregates.

5.5.3. Work of Cohesion

Figure 37 represents the cohesive energy of the asphalt binder samples, which is twice the total SFE. Higher work of cohesive indicates better potentials of strong bonding of the binder material, which means more energy is needed to break its cohesive bonds and higher resistance to moisture damage *(9)*. Figure 37 also shows that modified asphalt binders have higher work of cohesion than unmodified binders, which means modified binders have stiffer bonding and better resistance to moisture damage. For source 1 binders, the highest cohesion energy was observed for unaged S1B3 binder, which is a combination of PPA- and SBS-modified binder. Similarly, in source 2, S2B3 possesses an increased work of cohesion compared to the other binders from source 2.

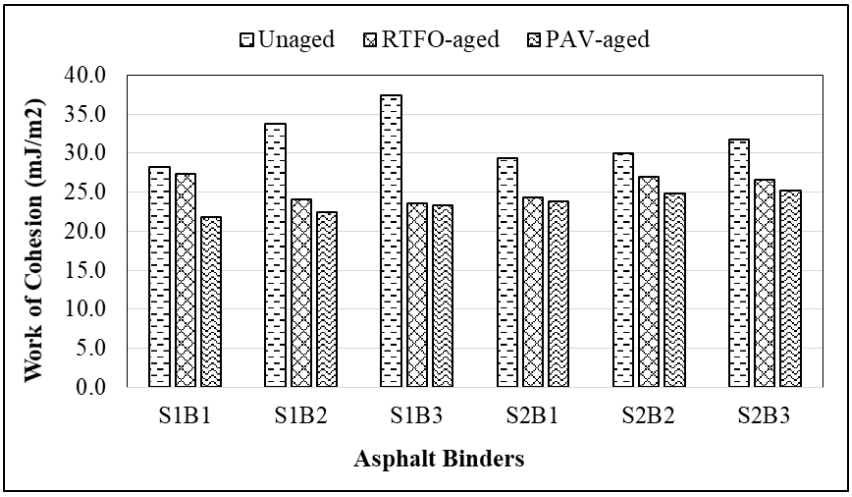

Figure 37. Work of Cohesion of Asphalt Binders under Different Aging Conditions.

An interesting finding from Figure 37 is that the RTFO and PAV aging decrease the cohesion energy more than the unaged binders, which means the aged binders are easy to crack. A small work of cohesion indicates that only a little work is required to create a unit area crack within the binder.

5.5.4. Work of Adhesion

As mentioned earlier, for an Asphalt Concrete (AC) mix to be durable and resistant to moisture damage, the work of cohesion and the work of adhesion should be as high as possible. A higher magnitude of these parameters implies that more energy is required to initiate a cohesive failure and adhesive failure in the AC mixture. Tables 13 through 15 represent the work of adhesion of the selected six types of binders and four types of aggregates combinations in different aging conditions. It is evident from Tables 13 to 15 that the adhesion values decrease with the aging of asphalt binders. Aging makes the binders stiffer so the adhesion values decrease with RTFO and PAV aging.

Table 13 shows the work of adhesion of unaged asphalt binders and aggregates. Both dry and wet conditioned adhesion values are calculated by using Equation 6 and Equation 7. Among the four aggregates, dolomite has the highest work of adhesion with the binders, and sandstone has the lowest adhesion value. Limestone and gravel are in between them. It is also found from Table 13 that the modification of binders increases the adhesion values. Here, the unmodified S1B1 binder and dolomite combination has the adhesion (dry) value of 71.04 mJ/m^2, whereas the PPA and SBS modified S1B3 and dolomite combination has a higher adhesion (dry) value of 75.13 mJ/m^2. A

similar trend is also observed for the other binder-aggregate combinations. Another interesting finding from Table 13 is that the adhesion (wet) values are less than adhesion (dry) values for dolomite, limestone, gravel, and sandstone with all the binder combinations except the S1B1 binder. The higher adhesion (wet) value means the unmodified S1B1 binder and aggregate combination is more susceptible to moisture-induced damage.

(Unaged)

Table 13. Work of Adhesion of Unaged Asphalt Binders and Aggregates.

Asphalt Binders	Sandstone Adhesion Dry (mJ/m^2)	Sandstone Adhesion Wet (mJ/m^2)	Gravel Adhesion Dry (mJ/m^2)	Gravel Adhesion Wet (mJ/m^2)	Dolomite Adhesion Dry (mJ/m^2)	Dolomite Adhesion Wet (mJ/m^2)	Limestone Adhesion Dry (mJ/m^2)	Limestone Adhesion Wet (mJ/m^2)
S1B1	62.76	74.11	66.56	72.11	71.04	69.74	68.53	71.08
S1B2	64.08	59.60	67.51	56.95	71.78	53.80	69.31	55.57
S1B3	67.10	58.57	70.68	56.02	75.13	52.97	72.55	54.69
S2B1	60.24	60.89	63.50	58.11	67.53	54.83	65.20	56.67
S2B2	60.82	60.71	64.10	57.95	68.17	54.69	65.82	56.52
S2B3	62.30	60.17	65.65	57.46	69.81	54.25	67.40	56.06

Table 14 represents the work of adhesion (mJ/m^2) of RTFO-aged asphalt binders and aggregates combinations for both dry and wet conditions. Same as unaged binders, RTFO-aged binders have a similar trend of adhesion values. At the same time, adhesion values of RTFO-aged binder and aggregate combinations are less than unaged condition, which proves that the aging decreases the work of adhesion due to higher stiffness. Table 14 also shows that the adhesion (wet) values of sandstone and gravel are higher than adhesion (dry) values, which suggest that the combinations of RTFO-aged asphalt binders and these two aggregates are exposed to stripping and moisture damage.

(RTFO)

Table 14. Work of Adhesion of RTFO-aged Asphalt Binders and Aggregates.

Asphalt Binders	Sandstone Adhesion Dry (mJ/m^2)	Sandstone Adhesion Wet (mJ/m^2)	Gravel Adhesion Dry (mJ/m^2)	Gravel Adhesion Wet (mJ/m^2)	Dolomite Adhesion Dry (mJ/m^2)	Dolomite Adhesion Wet (mJ/m^2)	Limestone Adhesion Dry (mJ/m^2)	Limestone Adhesion Wet (mJ/m^2)
S1B1	61.89	74.91	65.67	72.90	70.11	70.52	67.63	71.86
S1B2	55.87	62.61	58.98	59.77	62.78	56.41	60.60	58.29
S1B3	55.16	63.40	58.23	60.52	61.98	57.15	59.83	59.04
S2B1	55.41	62.66	58.46	59.74	62.20	56.32	60.04	58.23
S2B2	58.02	61.68	61.17	58.84	65.07	55.49	62.82	57.37
S2B3	57.69	61.80	60.83	58.94	64.71	55.58	62.47	57.46

Table 15 represents the work of adhesion (mJ/m^2) of PAV-aged asphalt binders and aggregates combinations for both dry and wet conditions. Same as unaged and RTFO-aged binders, PAV-aged binders have an increasing trend of adhesion values due to modifications. At the same time,

adhesion values of PAV-aged binder and aggregate combinations are less than RTFO-aged and unaged condition, which means that the aging decreases the work of adhesion due to higher stiffness of the binders. Same as RTFO-aged binders, PAV-aged binders also show that the adhesion (wet) values of sandstone and gravel are higher than adhesion (dry) values, which means the combination of PAV-aged asphalt binders and these two aggregates are exposed to stripping and moisture damage.

(PAV)

Table 15. Work of Adhesion of PAV-aged Asphalt Binders and Aggregates.

Asphalt Binders	Sandstone Adhesion Dry (mJ/m^2)	Sandstone Adhesion Wet (mJ/m^2)	Gravel Adhesion Dry (mJ/m^2)	Gravel Adhesion Wet (mJ/m^2)	Dolomite Adhesion Dry (mJ/m^2)	Dolomite Adhesion Wet (mJ/m^2)	Limestone Adhesion Dry (mJ/m^2)	Limestone Adhesion Wet (mJ/m^2)
S1B1	52.92	63.63	55.85	60.64	59.45	57.14	57.38	59.09
S1B2	53.63	63.35	56.59	60.38	60.23	56.90	58.14	58.84
S1B3	54.52	63.00	57.52	60.05	61.21	56.60	59.09	58.53
S2B1	54.99	62.84	58.01	59.91	61.73	56.48	59.59	58.40
S2B2	55.93	62.45	58.99	59.54	62.76	56.13	60.59	58.04
S2B3	56.37	62.30	59.46	59.40	63.26	56.01	61.06	57.91

5.5.5. Compatibility Ratio

The compatibility ratio (CR) of a particular asphalt binder with aggregate is calculated using Equation 9. A higher compatibility ratio means the combination of that particular asphalt binder and aggregate is less vulnerable to moisture damage. Generally, the CR increases if the ΔG (dry) is higher than the ΔG (wet) of the asphalt binder with an aggregate *(14, 39-40)*. In particular, a CR value of less than 0.5 is considered to be very poor, whereas CR values of more than 0.5 signify good compatibility between binder and aggregates. To be more precise, if the CR value is greater than 1.5 the compatibility is rated “very good.” The range of CR between 0.5 and 1.5 means “good,” and CR values between 0.5 and 0.75 means “poor.” Furthermore, CR values less than 0.5 means “very poor” compatibility.

Figures 38 through 40 show the compatibility ratio of asphalt binders and aggregates combination in different aging conditions. Figure 38 shows the CR of unaged asphalt binders and aggregates. Dolomite with S1B3, S1B2, and S2B3 combinations show higher CR values which means good bonding and less vulnerable to moisture. At the same time, limestone with S1B1 or S1B2 has high CR values. However, sandstone and binder combinations have lower CR values. Among the 24 binder-aggregate combinations, sandstone with S1B1 has the lowest CR values. Here, dolomite with S1B3 has the highest CR value of 1.42, which is very good bonding. Limestone with S1B3 and dolomite with S1B2 have the CR value of 1.33, which is the second-highest CR value among the 24 combinations.

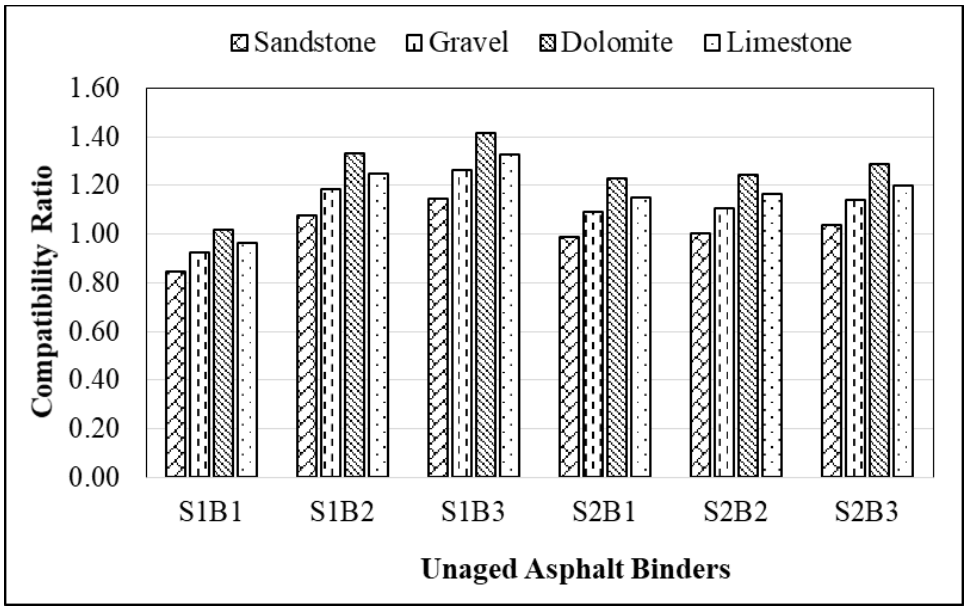

Figure 38. Compatibility Ratio of Unaged Asphalt Binders.

Figure 39 shows the CR of RTFO-aged asphalt binders and aggregates. It is found that the CR of each combination decreases a little bit for RTFO-aged binders comparing to unaged binders. For unaged binders, the highest CR is 1.42, whereas the highest CR for RTFO-aged binder is 1.17. Dolomite with S2B2, S2B3, and limestone with S2B2, S2B3 combinations are showing higher CR values. As before, sandstone with S1B1 has the lowest CR value for RTFO-aged binders.

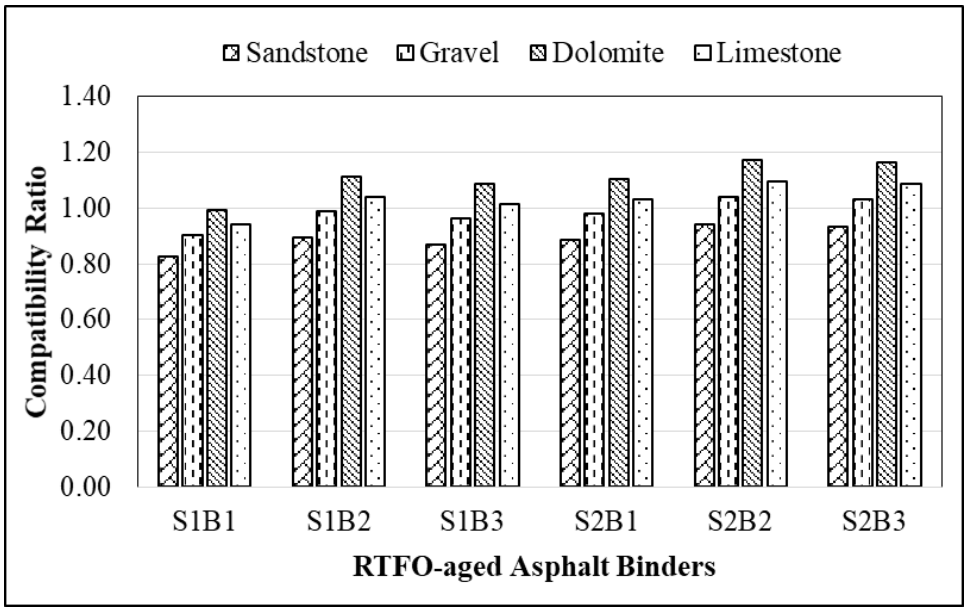

Figure 39. Compatibility Ratio of RTFO-aged Asphalt Binders.

Figure 40 shows the CR of PAV-aged asphalt binders and aggregates. It is found that the CR of each combination decreases for PAV-aged binders comparing to unaged and RTFO-aged binders. For unaged binders, the highest CR is 1.42, for RTFO-aged binder 1.17, whereas it is 1.12 for PAV-aged binders. It is evident that the aging of binders decreases the CR values because the

aggregates are in the same condition for all three cases. Dolomite with S2B3 is showing the highest CR value. Here, sandstone with S1B1 also has the lowest CR value for PAV-aged binders.

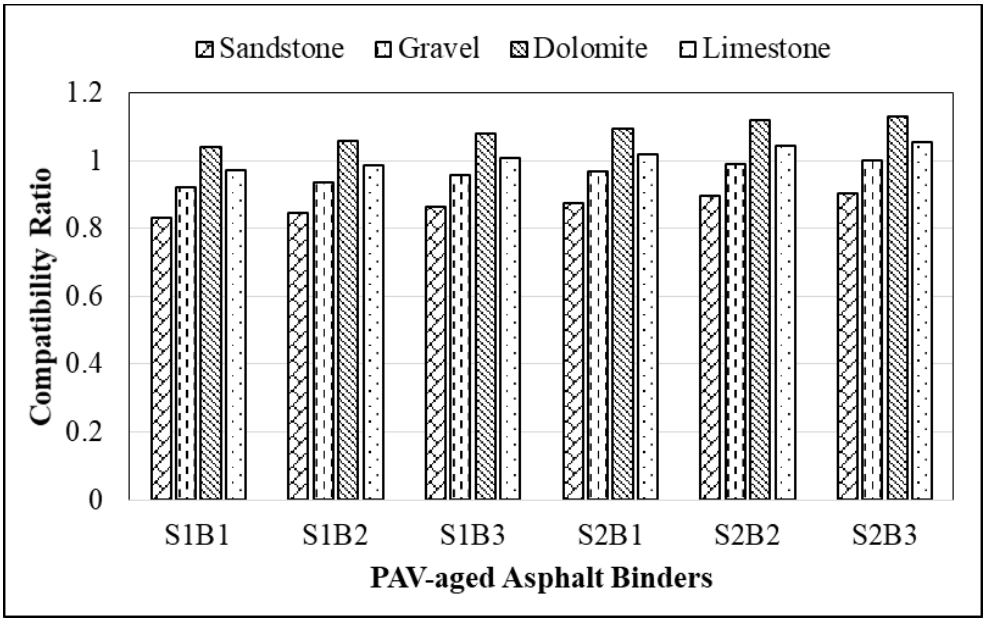

Figure 40. Compatibility Ratio of PAV-aged Asphalt Binders.

Based on Figures 38 to 40, it is found that dolomite and limestone with unaged, PPA, and SBS modified (PG 76-22) binders are showing very good compatibility. However, sandstone with PAV-aged unmodified (PG 64-22) is showing very poor compatibility.

The CR values of the recovered asphalt binders from the chip seal samples and the two types of aggregates (dolomite and limestone) used in these projects were also estimated. The CR values of these two types of aggregate-binder systems were about 1.0 (from 0.98 to 1.01), and there was no statistically significant difference between the CR values.

5.6. AFM Test Results

The AFM tests were conducted on unaged, short-term aged (RTFO), and long-term aged (PAV) binder samples to characterize the surface topography and the mechanical properties of the asphalt binder. Figure 41 shows the typical AFM-based maps of the surface morphology (roughness) of S1B1 (PG 64-22) binder samples in the top row, whereas S1B2 (SBS-modified PG 70-22) and S1B3 (PPA plus SBS-modified PG 76-22) binder samples are shown in the middle row and bottom row, respectively. On the other hand, the aging conditions of the corresponding binder samples are shown in the three columns where the unaged, RTFO, and PAV aging are shown in the first, middle, and last columns, respectively. The same styles are followed in Figures 42 through 44 for the representation of the AFM maps in the later section.

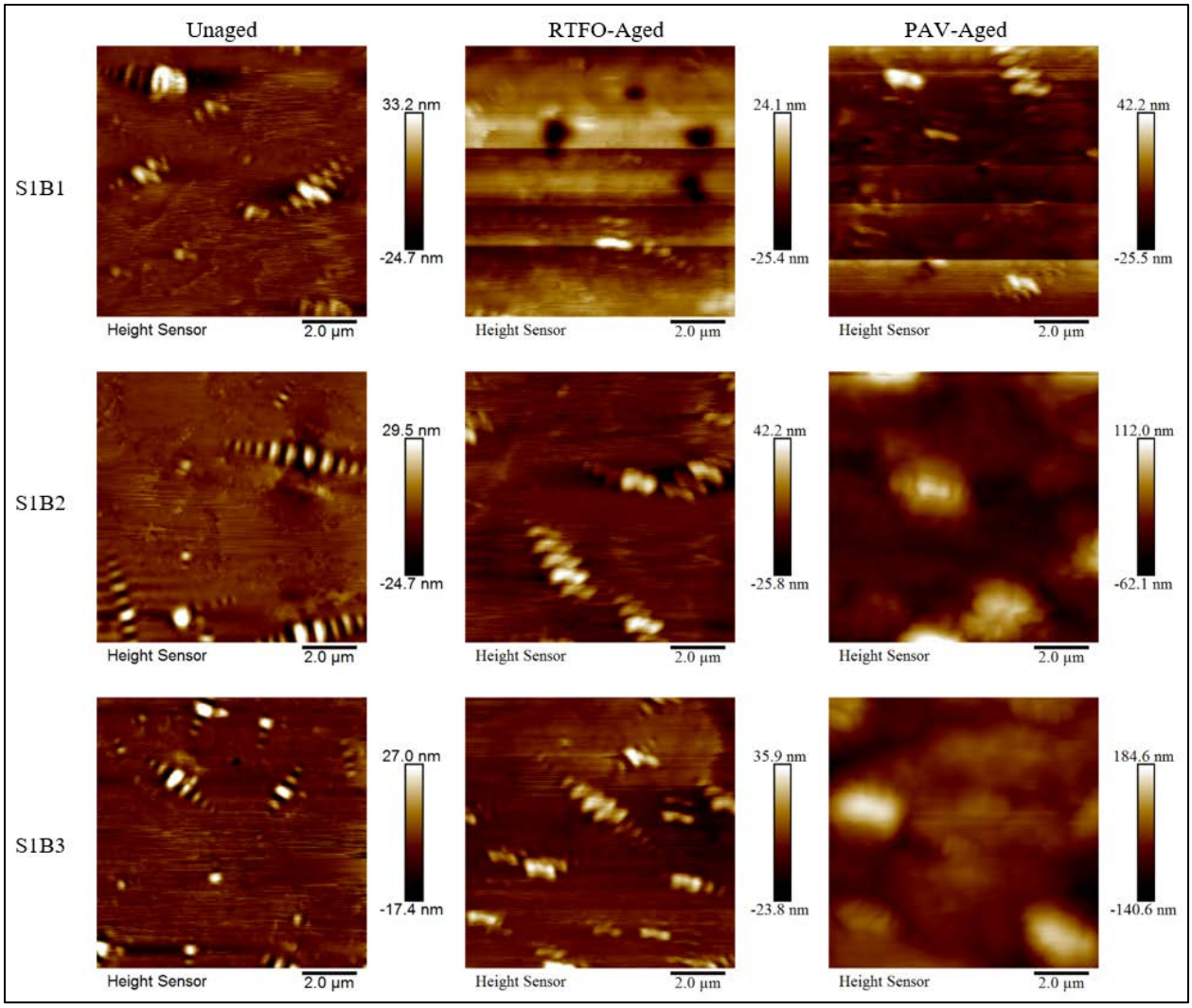

Figure 41. Typical AFM-based Maps of the surface roughness (nm) of Source 1 Binders.

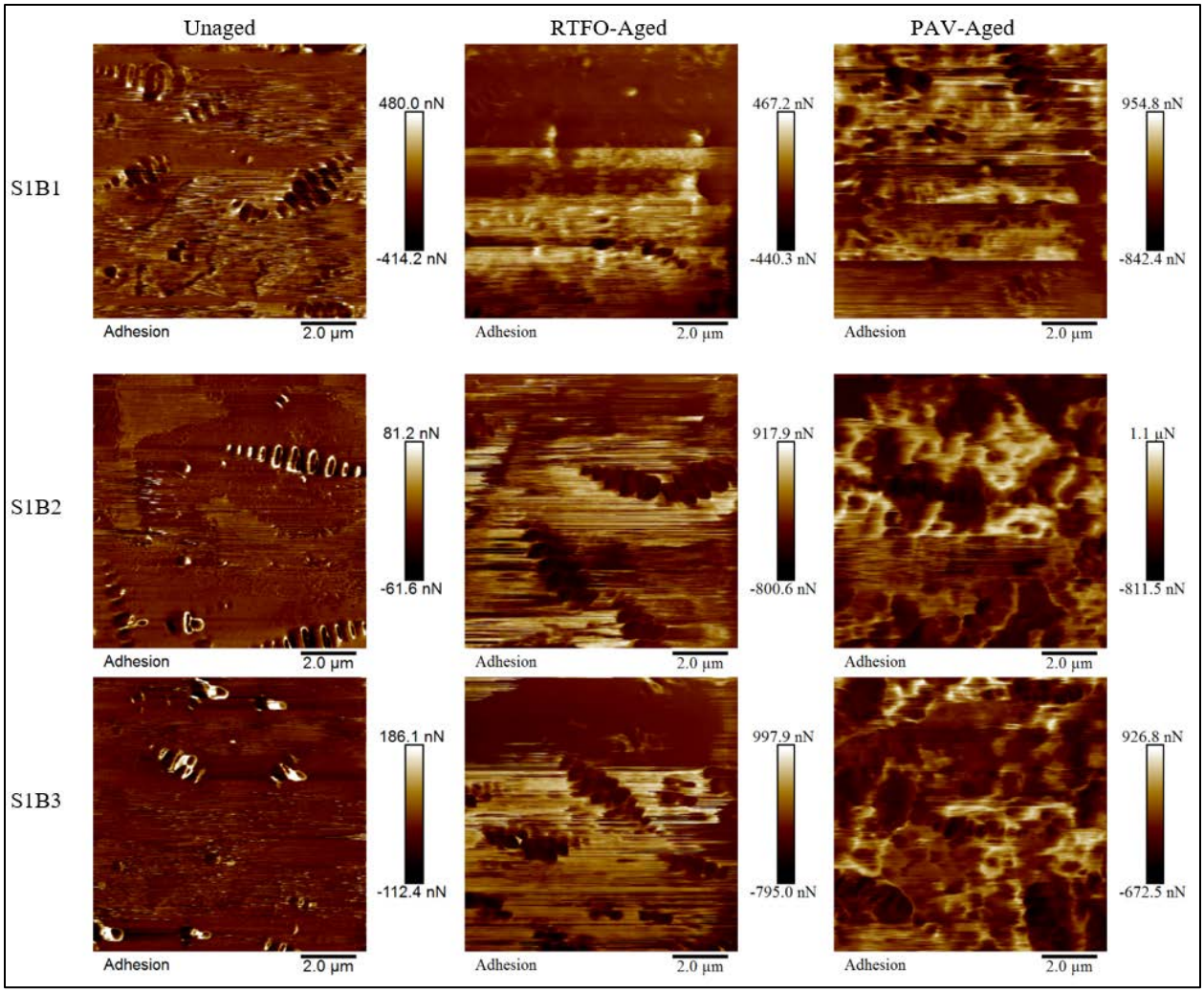

Figure 42. Typical AFM-based Maps of the Adhesion Energy (nN) of Source 1 Binders.

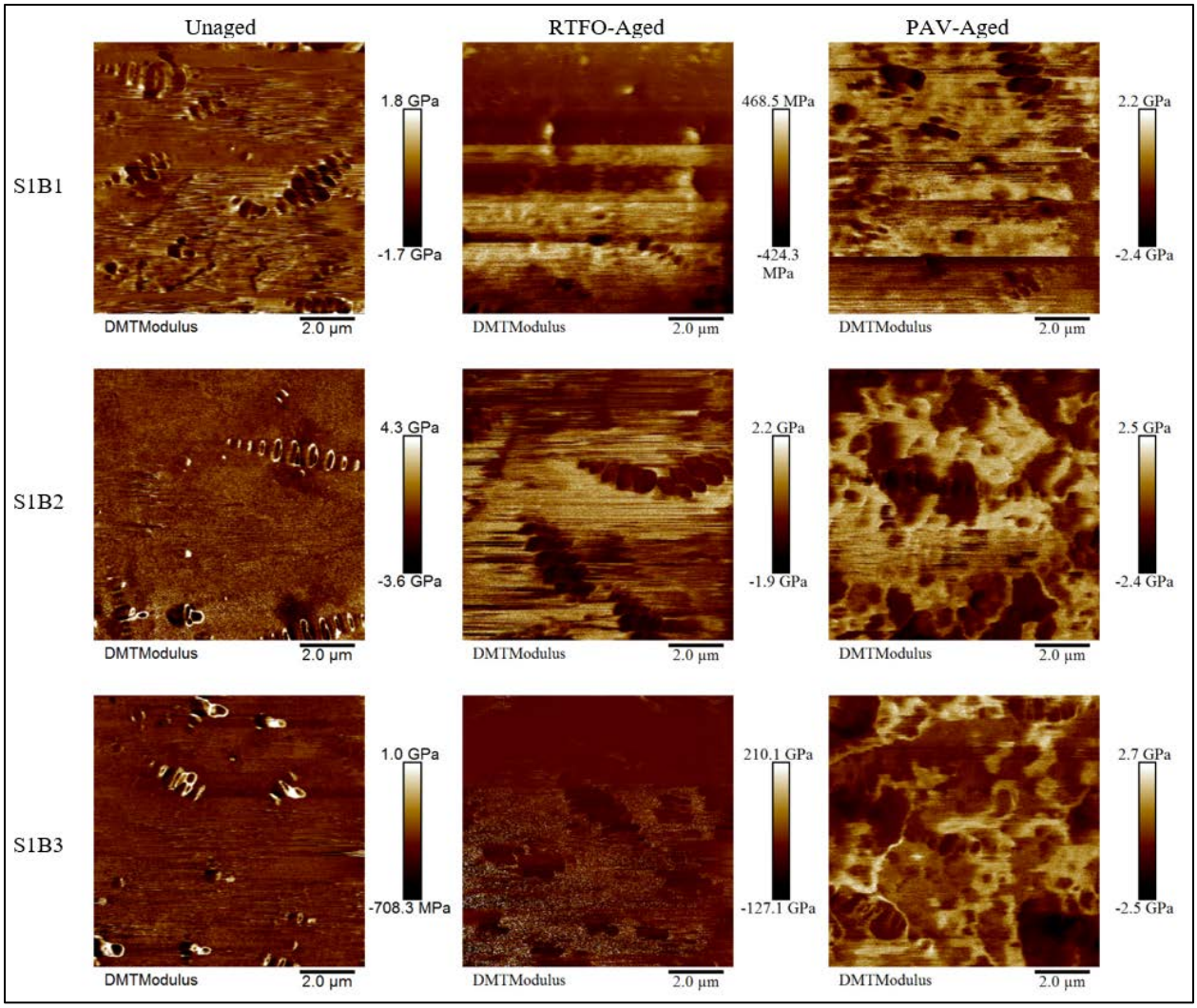

Figure 43. Typical AFM-based Maps of the DMT Modulus (MPa) of Source 1 Binders.

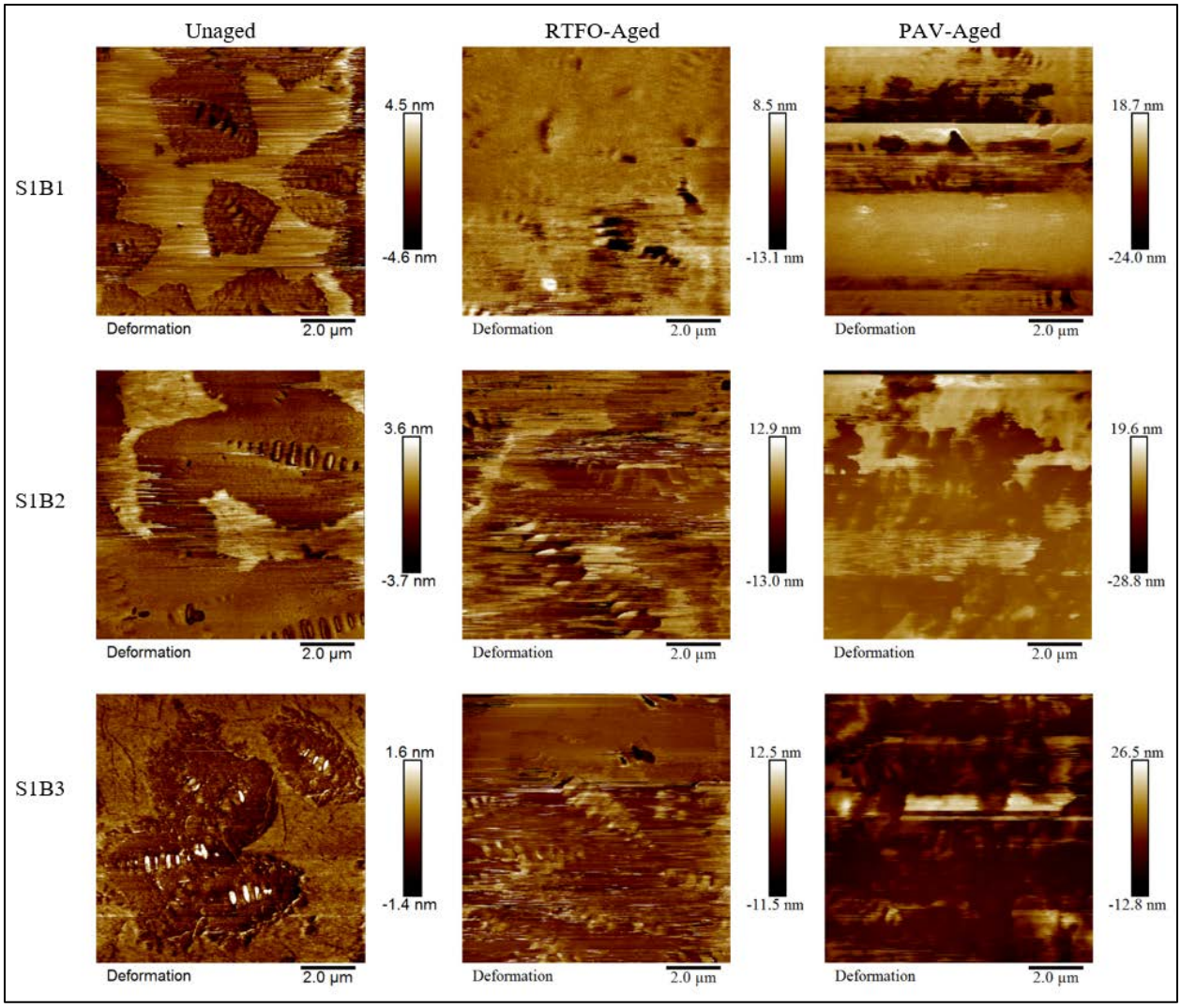

Figure 44. Typical AFM-based Maps of the Deformation (nm) of Source 1 Binders.

As shown in Figure 41, the AFM test results revealed three distinct phases (e.g., dispersed or Catena, interstitial or Peri, and matrix or Perpetua in unaged binder samples (*26-28, 31-32*). The morphological changes due to the short- and long-term aging of the binder samples are visible in Figure 41. In most of the cases, the bee-like structures appeared in the unaged asphalt binders which were significantly changed in size, decreased in numbers, and sometimes also dispersed due to the aging of the samples. Moreover, the summary of the binder's surface roughness values is presented in Table 16. From Table 16, it is found that the overall average surface roughness values were significantly increased for aged samples compared to their respective unaged samples. Among all tested binders, the PAV samples showed higher surface roughness values than RTFO samples for both S1 and S2. It is also noted that the binder samples modified with either SBS or SBS plus PPA showed the maximum values of roughness in the case of both RTFO- and PAV-aged samples.

Table 16. AFM Test Results of Source 1 and Source 2 Asphalt Binders.

Binder Type	Aging Condition	Roughness (nm)	Std. Error	Adhesion Force (nN)	Std. Error	DMT Modulus (MPa)	Std. Error	Deforma-tion (nm)	Std. Error
S1B1	Unaged	5.45	1.04	38	10.64	117	11.36	11.08	0.98
S1B1	RTFO	6.81	0.17	188	3.21	136	4.10	6.07	0.73
S1B1	PAV	9.55	0.47	113	5.81	740	8.45	4.74	0.20
S1B2	Unaged	4.47	1.51	76	2.04	318	22.26	6.1	0.21
S1B2	RTFO	9.67	0.31	237	17.09	615	12.81	5.09	0.56
S1B2	PAV	26.37	1.21	210	16.27	923	9.74	3.91	0.22
S1B3	Unaged	4.60	0.82	91	3.81	468	27.43	5.81	0.59
S1B3	RTFO	8.28	0.17	252	12.13	700	14.29	4.31	0.66
S1B3	PAV	37.30	1.76	215	2.73	750	20.43	2.59	0.66
S2B1	Unaged	1.99	0.34	35	1.25	112	17.63	9.48	0.91
S2B1	RTFO	9.51	0.73	152	8.01	215	6.74	5.86	0.62
S2B1	PAV	13.47	0.41	101	4.81	907	10.40	4.8	0.41
S2B2	Unaged	4.90	1.33	61	7.63	360	32.10	5.82	0.59
S2B2	RTFO	9.07	0.23	224	3.79	685	30.09	4.81	0.86
S2B2	PAV	25.93	2.18	205	5.55	732	6.12	3.44	0.71
S2B3	Unaged	4.27	0.65	83	5.90	571	4.84	4.9	0.52
S2B3	RTFO	10.27	0.47	243	5.13	668	11.57	3.97	0.48
S2B3	PAV	18.77	0.52	145	4.91	764	2.60	2.95	0.54

Figure 42 shows the typical AFM maps of the adhesion force (nN) values of all the asphalt binders from both sources (S1 and S2) evaluated in the study. Based on the analysis of the AFM test results, the adhesion forces for all binders are estimated, quantified, and presented their comparisons in Table 16.

According to Table 16, it is found that the average adhesion values were significantly increased in all RTFO- and PAV-aged binder samples than the corresponding unaged binders (32). The unaged binders had the adhesion forces varying from 35 nN to 91 nN while RTFO- and PAV-aged binder showed a range of 152 nN to 252 nN, and 101 nN to 215 nN, respectively. Compared to the unaged binders, the RTFO aged binders showed the highest increment rate in adhesion forces, whereas the PAV aged had a lower increasing rate (1.7 nN to 3.4 nN). Based on the AFM test results, it is evident that the adhesion forces are increased with the increment of binders' modification and their grades regardless of all aging conditions. For instance, the adhesion force of the S1B1 (Control) binder was found to be 35 nN, whereas the value of 76 nN and 91 nN were found for S1B2 (SBS-modified PG 70-22) and S1B3 (SBS plus PPA-modified PG 76-22) binder samples, respectively. A similar pattern is also noticed for S2 binder samples.

Figure 43 shows the typical AFM maps of the DMT modulus (MPa) of all the binders tested in this study. As seen from Figure 43 and Table 16, the modulus values were increased in RTFO aged binders, which further increased in the PAV-aged samples (32). This increasing pattern is noticed in the case of all binder samples tested in this study. Among all tested binders, it is found that the

modulus values varied from 112 MPa to 571 MPa for unaged asphalt binders, 136 MPa to 700 MPa for RTFO-aged asphalt binder, and 732 MPa to 932 MPa for PAV-aged asphalt binders. The average modulus values of RTFO- and PAV-aged asphalt binders were found to be increased by 1.2 to 1.9 times, and 1.3 to 8.1 times compared to unaged asphalt binder, which shows similar adhesion values compared to the unaged binder. It is also evident that, among all PAV-aged binders, the control binders from both sources (S1B1 and S2B1) showed the highest increment of modulus values.

Figure 44 shows the typical values of the deformation (nm) values of all the tested binders in this study. Based on Figure 44 and Table 16, it is found that the deformation values were decreased due to the aging of the binder samples. The RTFO-aged binders showed a reduced deformation compared to their corresponding unaged binders which further decreased in the case of PAV aged binders. This decreasing trend in deformation values was observed among all tested binders, irrespective of the binders' sources and grades. For example, for S1 binders, it is observed that the deformation values of S1B1, S1B2, and S1B3 binders were found to be 11.08 nm, 6.1 nm, and 5.81 nm, respectively for unaged binders, whereas these values are 6.07 nm, 5.09 nm, and 4.31 nm for RTFO-aged binders; and 4.74 nm, 3.91 nm, and 2.59 nm for PAV aged binders. A similar trend in deformation is also found among unaged and RTFO and PAV-aged binders from S2. Moreover, the AFM test results showed that the SBS modified binders (S1B2 and S2B2) had the lowest reduction (17%) in the deformation values for RTFO-aged binder samples compared to the corresponding unaged binders. Similarly, for PAV-aged binders, S1B2 and S2B2 showed a reduction of 36% and 41 % in deformation values, respectively.

5.7. Texas Boiling Test

Texas Boiling test is widely used for measuring the moisture damage of an asphalt mix for its simple procedure that takes very little time compared to the other test methods. The stripping of asphalt binders is measured by visual observation according to the TTI guidelines. Figure 45 shows the procedurally coated aggregate samples before and after the boiling test. In this study, four types of aggregates with six types of asphalt binders were coated separately and tested for Texas Boiling. The collected two chip seal samples were also tested for determining the percentage of asphalt retention. The chip seal samples were heated and loose samples were prepared. After cooling down, the loose samples were poured into the boiling water and tested for 10 minutes.

Figure 45. Texas Boiling Test.

In this test, moisture susceptibility of the asphalt mixes is determined based on the percentage of the asphalt retention, which is shown in Table 17. It is noted that PG 64-22 binders (S1B1 and S2B1) for both sources showed a lower percentage of asphalt retention after the boiling test compared to any other binder used in this study. On the other hand, the higher asphalt retention rates were found for S1B3 and S2B3 (PPA plus SBS-modified binders) from S1 and S2. Among the four aggregates, limestone and dolomite show more percentage of retention than the other two aggregates. Here, sandstone shows the lowest percentage of asphalt retention (only 10%-40%), which is rated "very poor." Based on the test results, it is evident that sandstone is more moisture susceptible and exposed to stripping.

The Texas Boiling test results of chip seal samples collected from the two roadways reveal that the sample collected from Site 1 (Highway 358 in Craighead Co.) had significantly lower asphalt retention of 60% compared to Site 2 (Highway 312 in Mississippi Co.), which had an 80% of retention (Table 17). As mentioned earlier, the visual inspection results also suggested Site 1 being more deteriorated than Site 2.

Table 17. Retention of Asphalt Binders (%) after the Texas Boiling Test.

Asphalt Binder	Sandstone	Gravel	Limestone	Dolomite
S1B1 (PG 64-22)	10	40	80	60
S1B2 (PG 70-22)	30	50	90	70
S1B3 (PG 76-22)	40	60	90	90
S2B1 (PG 64-22)	10	40	80	60
S2B2 (PG 70-22)	30	60	90	80
S2B3 (PG 76-22)	40	70	100	100
Site 1: Chip Seal 1	60			
Site 2: Chip Seal 2	80			

5.8. Ranking

Based on the properties of aggregates and binders obtained from laboratory test results, relative rankings are made. Tables 18 through 21 show these rankings. The lowest rank means the aggregate, binder, or binder-aggregate system is the best among all combinations, and vice versa.

5.8.1. Ranking of Aggregates

The rankings of the aggregates are conducted based on the aggregates' properties. Here, the test results of specific gravity, absorption, LA abrasion, soundness, and pH are considered for building the ranks. For specific gravity, the highest value of specific gravity is considered as Rank 1. For absorption, the lowest percentage of absorption is considered as Rank 1. Similarly, for the LA abrasion and soundness test, the lowest percentage of loss is considered as Rank 1. However, for the pH of aggregates, the highest pH value is considered as Rank 1 as the asphalt binder is generally acidic. Table 18 represents the relative rankings of the tested four aggregates.

Table 18. Ranking of Aggregates based on its Properties.

Aggregate Type	Specific Gravity	Absorption (%)	Loss (%) for LA Abrasion	Loss (%) for Soundness Test	pH
Limestone	3	1	3	2	1
Dolomite	1	2	2	1	2
Sandstone	4	4	4	4	3
Gravel	2	3	1	3	4

5.8.2. Ranking of Asphalt Binders

The rankings of the asphalt binders are conducted based on the binder's properties. Here, the pH, work of cohesion, and adhesion energy are considered for preparing the ranking. For the pH-based ranking process, the lowest value of pH is considered as Rank 1, assuming that aggregates will be basic. For the work of cohesion, its highest value is considered as Rank 1. Similarly, for the work of adhesion, its highest value is considered as Rank 1.

Table 19. Rankings of Asphalt Binders.

Asphalt Binders	Rank based on pH	SD-based Work of Cohesion (mJ/m^2)	SD-based Rank	AFM-based Adhesion Force (nN)	AFM-based Rank
S1B1	5	28.24	6	38	5
S1B2	4	33.76	2	76	3
S1B3	1	37.40	1	91	1
S2B1	3	29.39	5	35	6
S2B2	2	30.03	4	61	4
S2B3	1	31.69	3	83	2

5.8.3. Ranking of Asphalt-Aggregate Combinations

The main objective of this research is to find out suitable asphalt binder-aggregate combination to reduce stripping and moisture damage. The compatibility ratio is a very good parameter to determine the most suitable combination. The highest CR value is considered as Rank 1. Table 20 shows the ranking of binder-aggregate combinations based on their CR values. According to Table 20, it is found that dolomite with SBS modified S2B2 binder has the highest CR value and ranked No. 1, and dolomite with S2B3 binder is ranked as No. 2. Here, 24 combinations are ranked based on their CR values.

Table 20. Ranking of Asphalt Binder-Aggregate Combinations based on Compatibility Ratio.

Binder-Aggregate Combination	Rank
Dolomite-S2B2	1
Dolomite-S2B3	2
Dolomite-S1B2	3
Dolomite-S2B1 & Limestone-S2B2	4
Limestone-S2B3	5
Dolomite-S1B3	6
Limestone-S1B2 & Gravel-S2B2	7
Limestone-S2B1 & Gravel S2B3	8
Limestone-S1B3	9
Dolomite-S1B1 & Gravel -S1B2	10
Gravel-S2B1	11
Gravel-S1B3	12
Limestone-S1B1 & Sandstone-S2B2	13
Sandstone-S2B3	14
Gravel-S1B1	15
Sandstone-S1B2	16
Sandstone-S2B1	17
Sandstone-S1B3	18
Sandstone-S1B1	19

In this study, the percentage of retained asphalt binders after the Texas Boiling Test is used for making the rank of binder-aggregate combinations. The highest percent retention is considered as Rank 1. Table 21 shows the ranking of 24 combinations, and it is found that dolomite and limestone with S2B3 are in Rank 1.

Table 21. Ranking of Binder-Aggregate Combinations based on the Texas Boiling Test.

Binder-Aggregate Combination	Rank
Dolomite-S2B3 and Limestone-S2B3	1
Limestone-S1B2, Limestone-S1B3, Limestone-S2B2, and Dolomite-S1B3	2
Dolomite-S2B2, Limestone-S1B1, and Limestone-S2B1	3
Dolomite-S1B2 and Gravel-S2B3	4
Dolomite-S1B1, Dolomite-S2B1, and Gravel-S2B2	5
Gravel-S1B2	6
Gravel-S1B1, Gravel-S1B2, Sandstone-S1B3, and Sandstone-S2B3	7
Sandstone-S1B2 and Sandstone-S2B2	8
Sandstone-S1B1 and Sandstone-S2B1	9

From Tables 20 and 21, it is evident that dolomite and sandstone are showing strong bonding with modified (PG 70-22 and PG 76-22) asphalt binders, and gravel is showing moderate bonding. However, sandstone is showing very weak bonding with the asphalt binders.

6. CONCLUSIONS

The main goal of this study was to assess the durability of selected aggregates throughout Arkansas and their compatibility with asphalt binders from two different crude sources. To achieve the goal of this study, physical and mechanical tests of aggregates were performed in the laboratory. Besides the conventional test methods, some fundamental science-based advanced tests for asphalt binders were also included in the test plan. Asphalt binder samples used for this study were collected from two different sources (S1 and S2). The tested binders included unmodified (PG 64-22) and modified (PG 70-22 and PG 76-22) asphalt binders. The additives used in the modified binders were styrene-butadiene-styrene (SBS), and a combination of PPA and SBS. Besides, four types of ARDOT certified mineral aggregates from four different quarries are used in this study. Furthermore, asphalt samples were collected from two recently constructed chip seal projects in Arkansas, and the asphalt binder and aggregates recovered from them were tested in the laboratory.

To fulfill the objectives of this project, a series of laboratory tests were conducted and test data were analyzed to draw meaningful conclusions and recommendations. Physical property tests (e.g., specific gravity, absorption), mechanical property tests (e.g., LA abrasion, soundness test), and chemical property test (e.g., pH) of aggregates were conducted in the laboratory to evaluate the durability of selected aggregates. Superpave tests such as Rotational Viscometer, Dynamic Shear Rheometer (DSR), Rolling Thin-Film Oven (RTFO), Pressure-Aging Vessel (PAV), and Bending Beam Rheometer (BBR), were performed to evaluate the rheological properties of the tested binder samples. To evaluate the moisture resistance of the asphalt mixtures, the surface free energy (SFE) analysis has been included in this study. Additionally, the Texas Boiling test was conducted on loose mixture samples. An AFM tool was also used to characterize the microscopic morphology (roughness) and micro-mechanical properties (e.g., adhesion, DMT modulus, and deformation) of the asphalt binders at the molecular level.

Based on the test results, the following conclusions can be drawn:

1. Both specific gravity and absorption test results suggest that limestone ranks No. 1 while sandstone is the least one among all mineral aggregates tested in this study.
2. The LA abrasion test results showed that among four types of aggregates, gravel is the most durable (Rank 1) and sandstone is the least durable aggregate (Rank 4)
3. The Sulfate Resistance test shows that dolomite ranks No. 1 (best) while sandstone ranks No. 4 (worst) based on the percentage of loss. Sandstone is more vulnerable to weathering.
4. Based on pH test results, limestone has the highest value of pH, and SBS plus PPA modified S2B3 (PG 76-22) has the lowest value of pH. According to these results, limestone and S2B3 combination would be the best one.
5. The RV test results showed an increasing trend in viscosity of asphalt binders after using both SBS and SBS plus PPA. Polymer modifications make the binders more viscous.
6. DSR test results showed an increase in $G^*/\sin\delta$ values for SBS-modified binders from both sources under both unaged and RTFO aging conditions. Moreover, a higher rutting resistance is revealed in the case of modified binders. DSR test results also indicate that SBS-modified binder S1B2 is more fatigue resistant than the corresponding unmodified binder S1B1.
7. BBR test results showed that the lowest S-value for all binders from S1 is found for S1B3 (PPA plus SBS modified PG 76-22 binder) when then test temperature was -12 °C. For S2 binders, the lowest creep stiffness was observed for S2B2 (SSB-modified PG 70-22 binder).

8. The SFE analysis showed that modified binders had higher cohesion energy than unmodified asphalt binders. At the same time, the cohesion energy decreases with the aging of the binders. The highest work of adhesion was observed for dolomite and SBS+PPA-modified PG 76-22 binder from Source 1 (S1B3), and the lowest work of adhesion was found for sandstone and unmodified PG 64-22 binder from Source 2 (S2B1). Also, the compatibility analysis of asphalt binders with four different aggregates showed that dolomite with S1B3 had the highest CR, and limestone with S1B3 had the second-highest CR value, which means these two combinations are resistance to moisture-induced stripping. Whereas, sandstone with S1B1 had the lowest CR value and this combination is deemed vulnerable to moisture damage.
9. The AFM test is an effective tool to predict the moisture damage of the asphalt binders in both qualitatively and quantitatively at the atomic scale. AFM test results concluded that the SBS-modified binder had better resistance to moisture damage among all other binders. It is also observed that PPA plus SBS-modified binders from S1 showed sufficient moisture damage resistance.
10. Among all tests performed under the scope of this project, the Texas Boiling Test is simple, quick, and easy to perform for measuring the moisture susceptibility of the asphalt binder qualitatively. The Texas Boiling Test results revealed that the higher percentage of asphalt retained for PPA plus SBS-modified binders of both S1 and S2, indicating the higher moisture resistance with limestone and dolomite. While sandstone with unmodified asphalt binders had very little retention of asphalt binders.

REFERENCES

1. Copeland AR. Influence of moisture on bond strength of asphalt-aggregate systems (Doctoral dissertation), 2007.
2. Terrel, Ronald L., and John W. Shute. Summary report on water sensitivity. No. SHRP-A/IR-89-003, 1989.
3. Kanitpong K, Bahia HU. Role of adhesion and thin film tackiness of asphalt binders in moisture damage of HMA (with discussion). Journal of the Association of Asphalt Paving Technologists. 2003; 72.
4. Johnson DR, Freeman RB. Rehabilitation techniques for stripped asphalt pavements. Montana. Dept. of Transportation; 2002 Dec 1. Report No. FHWA/MT-002-003/8123.
5. Little DN, Bhasin A. Using surface energy measurements to select materials for asphalt pavement. 2006 Dec. NCHRP Project 9-37.
6. Masad E, Zollinger C, Bulut R, Little D, Lytton R, Khalid H, Davis R, Scarpas T, Fini E, Guarin A. Characterization of HMA moisture damage using surface energy and fracture properties. In Asphalt Paving Technology: Association of Asphalt Paving Technologists-Proceedings of the Technical Sessions 2006 Dec 21 (Vol. 75, pp. 713-754). Association of Asphalt Paving Technologist.
7. Cheng D, Little DN, Lytton RL, Holste JC. Surface energy measurement of asphalt and its application to predicting fatigue and healing in asphalt mixtures. Transportation Research Record. 2002; 1810(1):44-53.
8. Bhasin A, Little DN, Vasconcelos KL, Masad E. Surface free energy to identify moisture sensitivity of materials for asphalt mixes. Transportation Research Record. 2007 Jan; 2001(1):37-45.
9. Wasiuddin NM, Fogle CM, Zaman MM, O'Rear EA. Effect of antistrip additives on surface free energy characteristics of asphalt binders for moisture-induced damage potential. Journal of testing and evaluation. 2007 Jan 1; 35(1):36-44.
10. Hossain Z, Bhudhala A, Zaman M, O'Rear E, Cross S, Lewis S. Evaluation of the use of warm mix asphalt as a viable paving material in the United States. Cooperative Agreement: DTFH61-06-H-00044: Task. 2009 Nov; 3.
11. Van Oss CJ, Chaudhury MK, Good RJ. Monopolar surfaces. Advances in colloid and interface science. 1987 Jan 1; 28:35-64.
12. Buddhala A, Hossain Z, Wasiuddin NM, Zaman M, Edgar AO. Effects of an amine anti-stripping agent on moisture susceptibility of sasobit and aspha-min mixes by surface free energy analysis. Journal of Testing and Evaluation. 2012 Jan 11; 40(1):91-9.
13. Ghabchi R, Singh D, Zaman M. Evaluation of moisture susceptibility of asphalt mixes containing RAP and different types of aggregates and asphalt binders using the surface free energy method. Construction and Building Materials. 2014 Dec 30;73: 479-89.
14. Hossain Z, Bairgi B, Belshe M. Investigation of moisture damage resistance of GTR-modified asphalt binder by static contact angle measurements. Construction and Building Materials. 2015 Oct 1; 95:45-53.
15. Jie J, Yao H, Liu L, Suo Z, Zhai P, Yang X, You Z. Adhesion evaluation of asphalt-aggregate interface using surface free energy method. Applied Sciences. 2017 Feb; 7(2):156.

16. Little DN, Bhasin A. Using surface energy measurements to select materials for asphalt pavement. 2006 Dec. NCHRP Project 9-37.
17. Koc M. Development of testing protocols for direct measurements of contact angles on aggregate and asphalt binder surfaces using a sessile drop device (Doctoral dissertation, Oklahoma State University).
18. Susanna, L. What is surface free energy? Biolin Scientific: Surface Science Blog. Retrieved from https://www.biolinscientific.com/blog/what-is-surface-free-energy, Accessed July 10, 2020.
19. Baldi-Sevilla A, Aguiar-Moya JP, Vargas-Nordcbeck A, Loria-Salazar L. Effect of aggregate–bitumen compatibility on moisture susceptibility of asphalt mixtures. Road Materials and Pavement Design. 2017 May 8; 18(sup2):318-28.
20. Howson J, Masad EA, Bhasin A, Branco VC, Arambula E, Lytton R, Little D. System for the evaluation of moisture damage using fundamental material properties. Texas Transportation Institute, Texas A&M University. 2007 Mar.
21. Senadheera S, Tock RW, Hossain MS, Yazgan B, Das S. A testing and evaluation protocol to assess seal coat binder-aggregate compatibility. 2006 Jan.
22. Bahramian A. Evaluating surface energy components of asphalt binders using Wilhelmy Plate and Sessile Drop Techniques. 2012.
23. Hanz A. Test method to determine aggregate/asphalt adhesion properties and potential moisture damage. University of Wisconsin-Madison; 2007.
24. Al-Rawashdeh AS, Sargand S. Performance assessment of a warm asphalt binder in the presence of water by using surface free energy concepts and nanoscale techniques. Journal of materials in civil engineering. 2014 May 1; 26(5):803-11.
25. Kim SH, Jeong JH, Kim N. Use of surface free energy properties to predict moisture damage potential of asphalt concrete mixture in cyclic loading condition. KSCE Journal of Civil Engineering. 2003 Jul 1; 7(4):381-7.
26. Hossain Z, Roy S, Rashid F. Microscopic examination of rejuvenated binders with high reclaimed asphalts. Construction and Building Materials. 2020 Oct 10; 257:119490.
27. Roy S, Hossain Z. Use of molecular-level dissipated energy of asphalt binders to predict moisture effects on pavements. International Journal of Pavement Engineering. 2019 Nov 1:1-2.
28. Roy S, Hossain Z. Nanoscale quantification of moisture susceptibility of paving asphalts. In MATEC Web of Conferences 2019 (Vol. 271, p. 03005). EDP Sciences.
29. Nazzal, M.D., Holcombe, E., Kim, S.S., Abbas, A. and Kaya, S. Multi-scale evaluation of the effect of RAS on the fracture properties of asphalt mixtures. Construction and Building Materials, 2018; 175: 126-133.
30. Yang, Z., Zhang, X., Zhang, Z., Zou, B., Zhu, Z., Lu, G., Xu, W., Yu, J. and Yu, H. Effect of aging on chemical and rheological properties of bitumen. Polymers, 2018; 10(12):1345.
31. Hossain, Z., Rashid, F., and Roy, S., 2018. Multiscale evaluation of rejuvenated asphalt binders with a high RAP content. Transportation Research Board. https://trid.trb.org/view/1497197.
32. Roy S, Hossain Z. Nanoscale Study of the Influence of Short-Term and Long-Term Aging on Asphalt Binder's Properties. 2020 TranSET Conference, 2020 Sep 1-2. In Press.

33. Robertson RE, Branthaver JF, Harnsberger PM, Petersen JC, Dorrence SM, McKay JF, Turner TF, Pauli AT, Huang SC, Huh JD, Tauer JE. Fundamental properties of asphalts and modified asphalts, volume I: Interpretive report (No. FHWA-RD-99-212). 2001 Oct.
34. Wasiuddin NM, Zaman MM, O'Rear EA. Polymeric Aggregate Treatment Using Styrene-Butadiene Rubber (SBR) for Moisture-Induced Damage Potential. International Journal of Pavement Research & Technology. 2010 Jan 1;3(1).
35. Kittu AT, Bulut R, Harimkar S. Comparison of Contact Angle Measurements on Granite with Respect to Surface Roughness. 2013.
36. Kittu AT, Bulut R, Harimkar S. Comparison of Surface Energy Values of Limestone with Respect to Different 3D Surface Roughness Measurements. In Pavement Materials, Structures, and Performance 2014 (pp. 39-47).
37. Koc M, Bulut R. Evaluation of a warm mix asphalt additive using direct contact angle measurements. InInt. J. Pavements Conf 2013 (pp. 167-1).
38. Koc M, Bulut R. Assessment of a sessile drop device and a new testing approach measuring contact angles on aggregates and asphalt binders. Journal of materials in civil engineering. 2014 Mar 1;26(3):391-8.
39. Arabani M, Roshani H, Hamedi GH. Estimating moisture sensitivity of warm mix asphalt modified with zycosoil as an antistrip agent using surface free energy method. Journal of Materials in Civil Engineering. 2012 Jul 1;24(7):889-97.
40. Hefer AW, Bhasin A, Little DN. Bitumen surface energy characterization using a contact angle approach. Journal of Materials in Civil Engineering. 2006 Dec;18(6):759-67.

APPENDIX A: Aggregates' Properties

A_Table 1 Absorption (%) of Aggregates.

Aggregate Type	Absorption (%)	St. Error	Rank
Limestone	0.53	0.034	1
Dolomite	0.92	0.034	2
Sandstone	2.30	0.064	4
Gravel	1.39	0.056	3

A_Table 2 Specific Gravity of Aggregates.

Aggregate Type	Bulk dry Sp. Gr.	Bulk SSD Sp. Gr.	Apparent Sp. Gr.	Rank
Limestone	2.682	2.697	2.721	3
Dolomite	2.757	2.782	2.829	1
Sandstone	2.484	2.541	2.635	4
Gravel	2.715	2.752	2.821	2

A_Table 3 LA Abrasion test Results.

Aggregate Type	Loss	St. Error	Rank
Limestone	26.970	0.401	3
Dolomite	20.455	0.694	2
Sandstone	28.727	0.367	4
Gravel	17.515	0.774	1

A_Table 4 Soundness Test Results.

Aggregate Type	Loss (%)	Rank
Limestone	2.83	2
Dolomite	2.51	1
Sandstone	10.14	4
Gravel	3.64	3

A_Table 5 pH of Aggregates.

Aggregate Type	pH	St. Error	Rank
Limestone	8.84	0.057	1
Dolomite	8.43	0.030	2
Sandstone	7.82	0.045	3
Gravel	7.33	0.009	4

APPENDIX B: Asphalt Binder's Properties

B_Table 1 pH of Asphalt Binders.

Asphalt Binder	pH	Rank
S1B1	8.30	5
S1B2	6.90	4
S1B3	2.80	1
S2B1	6.20	3
S2B2	5.9	2
S2B3	2.8	1

APPENDIX C: Sample Preparation for OCA test

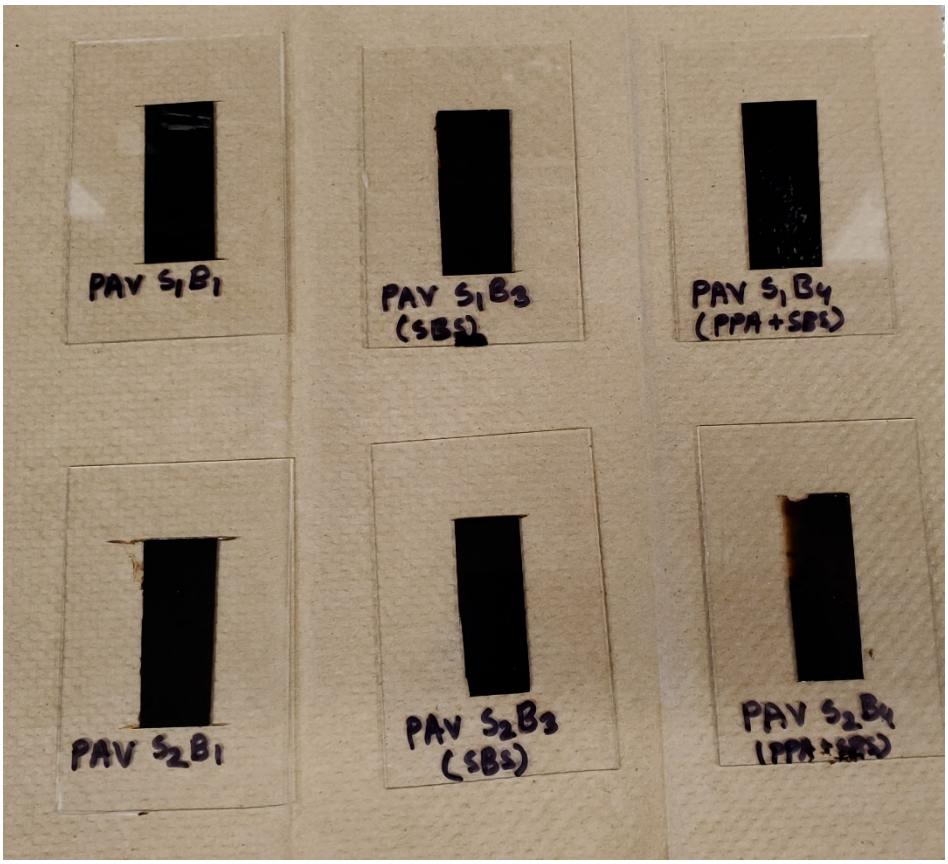

C_Figure 1 Binder Sample Preparation for OCA Test.